Norwegian University
of Life Sciences

Master's Thesis 2022 60 ECTS

Faculty of Biosciences

CRISPR/Cas9 based knockout of genes in SHK-1 cell line, to investigate their role in development of Infectious salmon anemia virus infection

Arvind Kurup
Master of Science in Animal Breeding and Genetics

Acknowledgements

Firstly, I would like to thank my supervisor, Guro Sandvik for having me as her master student and being the best supervisor that I could have asked for. I would like to thank her for always being so kind, supportive and positive. I would like to thank my co-supervisor Noman Reza for all the assistance and teaching. I would like to thank all the members of CIGENE, especially Tomasz, Jenny, Dominiki and Prabin for all the help and support. Special thanks to Erika.

I would like to thank Aurora Myhre for not only being an amazing lab partner but also a wonderful friend. I would like to specially thank Lars Aurstad for his valuable support. I would also like to thank my friends - Ashwin Sunilkumar, Omkar Tiware and Sneha Pillai for their invaluable companionship.

I would like to wholeheartedly thank Iben Andersen for being a mentor to me and looking out for me. I would also like to thank all the staff of Student's Information Centre of NMBU, especially – Benedikte, Trine, Tendai, Vilma, Megumi and Tonje. I would like to specially thank Sofia, for always helping me and being there for me.

I would like to thank Professor Dag Inge Våge and Elise Norberg for their valuable guidance and all the inspiring conversations.

Most of all, I would like to express my gratitude to my parents, Moly Kurup and Rajendra Kurup; and my brother, Ashwin Kurup, for all their love and support; without which nothing would be possible.

Arvind Kurup

Ås, August 2022.

Table of Contents

Abstract:

In recent years, we have realized the potential of aquaculture as an industry to meet the goal of rising global food demand in a cost-effective manner, rooted in sustainable and environment friendly practices. Atlantic salmon, as a fish, has a sizeable share in the Norwegian Aquaculture industry and plays a popular role in the Norwegian food culture. Out of the several diseases that affect the health of Atlantic salmon, the viral disease caused by Infectious Salmon Anemia virus is particularly notorious. It is a notifiable disease as per the World Organization for Animal Health and infection with ISAV has known to be difficult to control, causing epizootic episodes that threaten not only threaten the welfare of commercial salmons but also wild populations. Some of the challenges involved with control of the ISAV infections include a high mortality rate and lack of any treatment options – prophylactic or otherwise, leading to severe economic losses to the Norwegian aquaculture industry.

In this study we aimed to identify the genes involved in the development of ISAV infection. We investigated if at least one of the three genes- *TMEM199, WDR7* and *CCDC115* could be involved in the mechanism of infection for ISA virus. This was achieved by a CRISPR/Cas9 based knockout of the target genes followed by virus challenge study on SHK-1 cell line.

1 Introduction

1.1 The Atlantic salmon

Salmo salar (Linnaeus, 1758), also known as the Atlantic salmon is a ray-finned fish species belonging to the family Salmonidae (Near et al., 2012). Majority of the Atlantic salmon (*Salmo salar*) populations follow a life cycle which is anadromous in nature characterized by spending the early part of life in freshwater, migration to the sea for feeding and returning to the river for spawning activity (Kjærner-Semb et al., 2021). Atlantic Salmon is a popular food source and is considered an important part of the Norwegian food culture. According to FAO (2022), current worldwide framed salmon production is in the excess of 1000000 tonnes and Atlantic salmon constitutes more than 90% of the total farmed salmon market. Salmons also play a key role by acting as indicator species, reflecting the health of Pacific and North Atlantic river and coastal ecosystems (Lien et al., 2016).

Fish is considered a good nutritional source with high-quality proteins and vitamin D (Vikøren et al., 2017). Fish has been traditionally considered as a part of balanced diet and provides minerals, fat soluble vitamins like vitamin A, D and water-soluble vitamins like Niacin and vitamin B12, they also provide n-3 Poly unsaturated fatty acids or PUFAs like eicosapentaenoic acid and also docosahexaenoic acid (Atanasoff et al., 2013; Chiesa et al., 2016)

1.2 Aquaculture and contribution of Atlantic salmon to Norwegian GDP

By the year 2030, aquaculture production is projected to increase up to 106 million tonnes, with a growth of 22 % compared to the year 2020 and the projection for the share of farmed species in global aquaculture production and fisheries is 53 % for the year 2030, compared to 49% in the year 2020 (FAO,2022). Blue Transformation is a visionary strategy under the Food and Agriculture Organization of the United Nations, with an aim to enhance the aquatic food system's role to feed the growing world population and propose actions to ensure sustainable growth in aquaculture and fisheries with climate friendly choices. The General Assembly of United Nations has declared the year 2022 as the International Year of Artisanal Fisheries and Aquaculture – IYAFA 2022.

According to a study by Boyd and McNevin (2015), it was estimated that 0.17% of global land use was accounted for by aquaculture and water consumption was estimated to be 0.82%

of the total available renewable freshwater (Boyd et al., 2022). Estimated greenhouse gas emission by aquaculture was at 0.49% of the total global greenhouse emissions, in the year 2020 (MacLeod et al., 2020).

According to the Norwegian Seafood Council, Norway has exported a record 3.1 million tonnes of seafood with a value of NOK 120.8 billion in 2021, in which the biggest share of 81.4 billion NOK was by the Salmon ("Record high Norwegian seafood exports in 2021", 2022). All these factors, emphasize the role of Salmon in the Norwegian aquaculture industry and the importance of research on the health and well-being of Atlantic salmon, not only from a biological perspective but also from an economic perspective. 'Blue growth' is an initiative under the Norwegian Government - The Ministry of Trade, Industry and Fisheries to further develop and bring forth technological innovations and sustainability, especially in the Norwegian ocean industries which includes aquaculture.

1.3 Epidemiology of viral diseases of Atlantic salmon in Norway

Several feral and farmed populations of fish have been clinically diagnosed with diseases, including emerging diseases especially over the last decades; which has created large problems in the aquaculture industry and thereby warranting monitoring and disease surveillance programmes in many countries (Reinertsen & Haaland, 1995, as cited by Håstein et al., 2000). Compared to terrestrial animals, approaching the problem of infectious diseases in fish would be different due to the flowing water being an effective medium for transmission. (Håstein et al., 1999)

According to Institute of Marine Research, Bergen, substantial economic losses occur due to viral diseases of Atlantic Salmon in Norway causing a negative effect on the welfare of infected fish (Madhun, Bjørn et al., 2021). Some of the most common diseases of viral origin in salmon farming are Infectious salmon anaemia (ISA), caused by Infectious salmon anemia virus (ISAV), Infectious pancreatic necrosis (IPN), caused by IPN virus (IPNV), heart and skeletal muscle inflammation (HSMI), caused by piscine Orthoreovirus 1 (PRV1), cardiomyopathy syndrome (CMS), caused by piscine myocarditis virus (PMCV) and the pancreas disease (PD), caused by salmonid alphavirus (SAV) (Madhun, Bjørn et al., 2021). In terms of disease surveillance and control for aquatic animals, all Nordic countries have set up a national legislation with regulations which list the notifiable diseases of concern to countries (Håstein et al., 2001) . ISA is caused by ISAV, a characteristic disease of farmed Atlantic salmon which first recorded in Norway in the year 1984 (B. H. Dannevig et al., 2008)

Severe epizootics in fish populations have been encountered due to ISAV in Norway, Faroe Islands and Chile, subsequently leading to heavy economic losses for the aquaculture industry and compared to 1993, in recent years, Norway has been witnessing an increase of ISAV outbreaks along the coastline which highlights a growing issue for aquaculture industry and poses a risk of disease transmission between farms and between farms and wild populations. (Madhun, Bjørn et al., 2022).According to the World Organization for Animal Health (OIE), ISAV is a notifiable disease (Aamelfot et al., 2012).

Table 1.1: Table showing the number of ISAV outbreaks reported in Norwegian fish farms from the year 2017-2021 according to the Institute of marine Research, adapted from (Madhun, Bjørn et al.,2021).

	2017	**2018**	**2019**	**2020**	**2021**
ISA	14	13	10	23	25

1.3.1 Transmission of Infectious salmon anemia virus

Experimental infection studies have shown that ISA infection shows water borne transmission horizontally and there is a lack of evidence showing vertical transmission (OIE, 2021). However, a study by Nylund et al.,(2007) proposes a possibility of transgenerational or vertical transmission. Long distance spread of the disease has been attributed to transportation of infected smolt before shipping or also by ISAV contaminated well boats, this contamination of the boat can have two primary possibilities, one being previous transport of contaminated fish infected with ISAV or due to water from areas which have farms consisting of infected stock of fish (OIE, 2021). Epidemiological study states that the risk of ISAV spread is highly associated with horizontal transmission and human husbandry practices and transmission through sea lice and infected wild fish have also been proposed as possibilities in the category of horizontal disease transmission (OIE, 2021).

1.4 Introduction to Infectious salmon anemia virus (ISAV)

ISAV is the type species belonging to the genus *Isavirus* of the family *Orthomyxoviridae* (Gr. *Orthos*: standard, *myxo*: mucus). It is the only fish virus belonging to that family (Scott et al., 2011) . The virus has an optimum growth at a temperature of 15 ℃ and is adapted to cold-water salmonid fish (B. H. Dannevig et al., 2008). ISAV is classified as - type V virus of Baltimore classification system (Scott et al., 2011) and is a negative sense, single-stranded RNA virus (King et al., 2012).

1.4.1 Infectious salmon anemia virus variants

A work by Gagné & LeBlanc (2017), characterizes two groups of ISAV – European clade and the North American clade based on the sequence difference in partial sequence of genomic segment 6. The European variant is more widespread and shows more genetic variation and based on the presence or absence of deletion in the HPR (highly polymorphic region) of genomic segment 6, ISAV variants are classified as pathogenic or non-pathogenic (Kibenge et al., 2007; Nylund et al., 2007). HPRΔ variant is the only variant known to be growing in cell cultures (Ditlecadet et al., 2022).

According to Norwegian Food safety Authority (2020), the pathogenic type of ISAV is associated with disease outbreaks whereas the non-pathogenic strain (ISAV-HPR0) limits itself to sub-clinical infections and a positive PCR for ISAV-HPR0 (avirulent) is not notifiable according to legislation of Norway. According to OIE, both the strains are reportable, however ISAV-HPR0 (avirulent) is not generally notified due to absence of notification requirement as per the national legislation of Norway. (Jansen et al., 2022, p:3). Based on the presence or absence of deletion in the HPR (highly polymorphic region) of genomic segment 6, ISAV variants are classified as pathogenic or non-pathogenic (Ditlecadet et al., 2022). ISAV-HPR0 (avirulent) is assumed to be the precursor for all virulent strains that cause ISAV outbreaks (O.Dale, M. Hjortaas, S. Weli, 2013 and Christiansen et al.,2017). The nucleotide identity or similarity between the ISAV isolates (virulent and avirulent) is high overall and the highest variation is found in the HE gene and the virulence is determined by the nucleotide deletion in HPR (B. H. Dannevig et al., 2008)

A work by Christiansen et al., (2017), provided evidence of the functional and genetic evolution of ISAV-HPR0 variant (avirulent) to a low virulent HPRΔ variant in an Atlantic Salmon farm in the Faroe Islands. The results demonstrated the deletion in HPR of HE protein

and mutation in the F protein was required for the ISAV-HPR0 variant (avirulent) to gain virulent property and to also switch the cell tropism from localized infection of epithelium to a systemic infection characterizing endotheliotropism (Christiansen et al., 2017).

1.4.2 Infectious salmon anemia virus structure

The nucleotide sequence for ISAV consists of 8 genomic segments that code for at least ten proteins (Kibenge et al., 2007; Nylund et al., 2007) , which includes the 5' and 3' non coding sequence (Kulshreshtha et al., 2010)

A nucleoprotein (68 kilodalton) is encoded by genome segment 3, haemagglutinin-esterase (HE) (42 kilodalton) protein which is responsible for both receptor destroying activity and the receptor binding activity is encoded by genome segment 6, whereas the matrix protein (22 kilodalton) is encoded by genome segment 8 and a surface glycoprotein with putative fusion activity is encoded by genome segment 5; these comprise the four main structural proteins. (OIE, 2021).

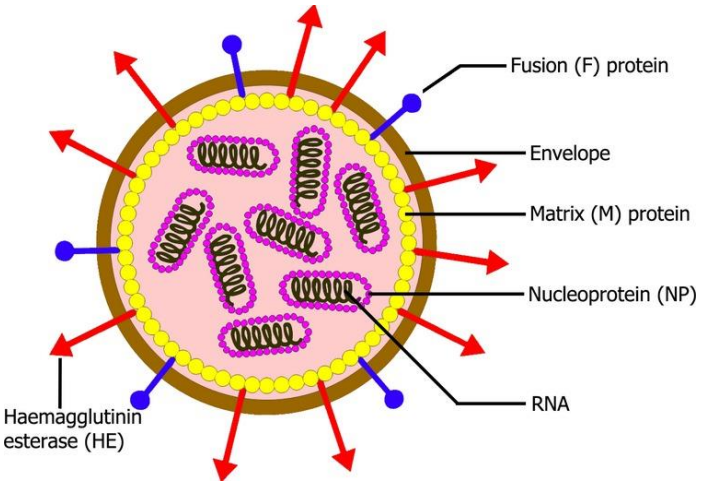

Figure 1.1: The structure of the Infectious Salmon anaemia virus particle. Image adapted from Aamelfot et al., (2014).

Viral polymerases are encoded for by genomic segment 1(PB2), segment 2 (PB1) and segment 4(PA) (Aamelfot et al., 2014). Genomic segment 7 and segment 8 are the two smallest segments and genomic segment 7 has two ORFs, ORF1 which codes for a protein with interferon Type 1 antagonistic property whereas ORF2 encodes nuclear export protein (NEP), whereas genomic segment 8 has two open reading frames, in which ORF1 is the smaller frame that codes for the matrix protein whereas ORF2 is the larger one that codes for

RNA-binding protein which is also possessing interferon type 1 antagonistic properties. (OIE, 2021).

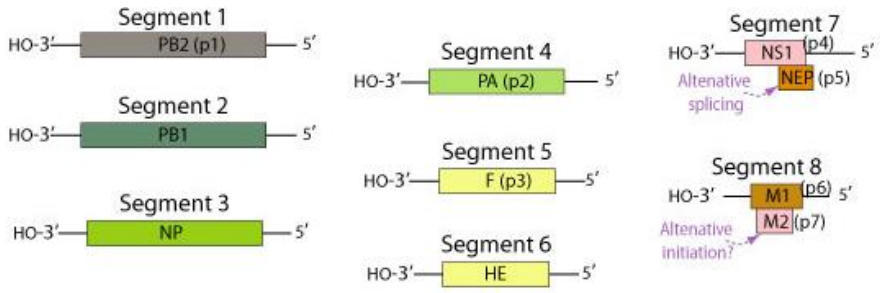

Figure 1.2: The genome segments of ISAV (Philippe Le Mercier, 2022).

1.4.3 Mechanism of ISAV entry and replication

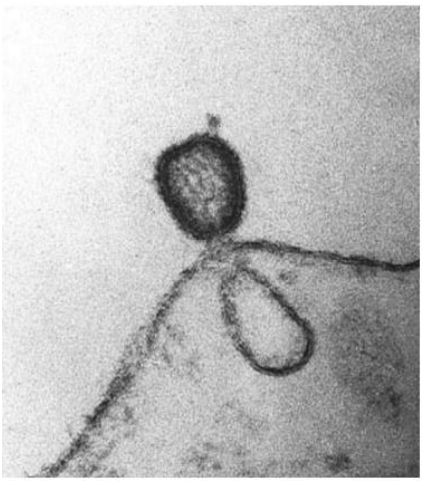

Figure 1.3: Electron microscope image showing ISAV invagination of host plasma membrane (Rimstad & Markussen, 2020).

The HE spikes of ISAV are trimeric in structure and are HE monomers which are embedded in the viral membrane and have control over the cleaving and receptor binding activities (Cook et al., 2017). 4-0-acetylated sialic acid is the preferred cellular receptor for ISAV (Hellebø et al., 2004). Endothelia cells shows high distribution of these receptors and are therefore main target for the ISAV attachment (Aamelfot et al., 2012; Rimstad & Markussen, 2020). Endocytosis mediated cellular uptake is induced when the viral HE glycoprotein attaches to the host cell surface receptor (Rimstad & Markussen, 2020).

The fusion of viral envelope and endosome membrane is facilitated by the structural modification of F glycoprotein which is induced by the acidic pH of the endosome (Eliassen et al. 2020; as cited in Rimstad & Markussen, 2020). Post the fusion, viral ribonucleoproteins and M1 proteins gain an entry into the cellular cytoplasm and the nuclear transport of the viral ribonucleoprotein is facilitated by the nuclear localization signal motifs that are present in PB1, PB2, PA as well as NP (Ramly et al., 2013; Rimstad & Markussen, 2020). Larger complexes make use of the nuclear machinery for entry and exit however, molecules with less molecular weight (< 40 kilodaltons) can passively diffuse through the nuclear pore (Rimstad & Markussen, 2020). The 3' end of genome segments of ISAV has 7 conserved nucleotides whereas 5' end has 8 conserved nucleotides, comparatively shorter than the Influenza A virus (Fourrier et al., 2014; Rimstad & Markussen, 2020). An important aspect of transcription is assumed to be pairing of the 5' and 3'ends of the virus to make double stranded , 'pan-handle' structures (Rimstad & Markussen, 2020; Sandvik et al., 2000).

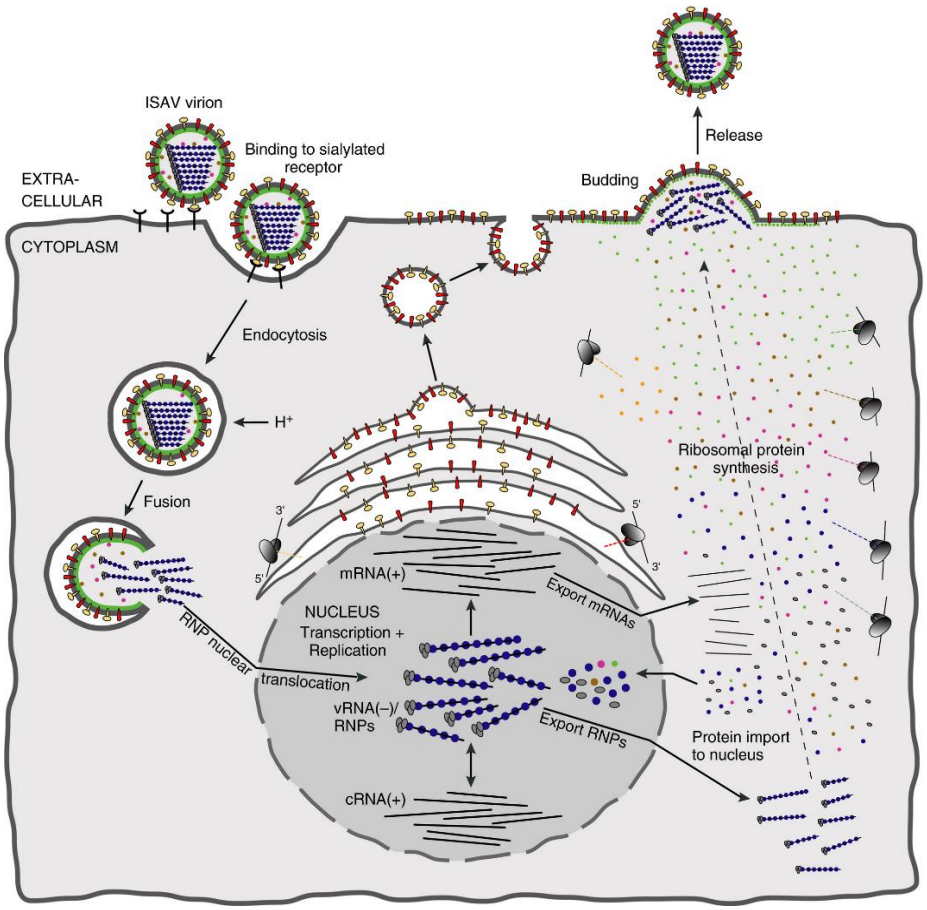

Figure 1.4: Pictorial representation of ISAV life cycle. Image adapted from Rimstad & Markussen,(2020).

ISAV genomes undergo transcription and replication in the nucleus and utilize the host cell splicing machinery (Rimstad & Markussen, 2020). The viral mRNAs have 5' ends which are capped and are 'stolen' from the nuclear mRNAs of the host cell and in this process 3' nucleotide of the viral RNA is lost (Rimstad & Markussen, 2020; Sandvik et al., 2000). This affects the transcription of host cells and the viral nuclear export protein (NEP) facilitates the nuclear export of the viral ribonucleoprotein from the host cell mediated by the Nuclear exporting signals (Ramly et al., 2013).

1.5 Disease presentation of ISAV infection in Atlantic Salmon

Characteristic clinical sign externally is appearance of pale gills except in cases involves stasis of blood in gills, distension of abdomen, exophthalmia, scale pocket oedema and presence of blood in the anterior eye chamber may be observed and staying true to the name, circulatory disturbances combined with anaemia is always presented clinically (OIE, 2021).

Figure 1.5a: Atlantic salmon with exopthalmia and pale gills post ISAV infection. Adapted from Godoy et al., (2008).

Macroscopic lesions may include haemorrhages of the parietal and visceral peritoneum, swim bladder oedema, accumulation of blood-tinged fluid in pericardial and peritoneal cavities etc. Microscopic lesions include erythrocytic thrombi in gills, presence of erythrocytes in central venous sinus. Accumulation of erythrocytes may also be seen in kidney glomeruli, focally in hepatic sinusoids, also in blood vessels of intestinal lamina propria prior to haemorrhage. Tubular necrosis and diffuse or multifocal interstitial haemorrhages in areas showing haemorrhages. Secondary haemorrhages of kidney and liver and erythrophagocytosis in spleen has been reported. (OIE, 2021)

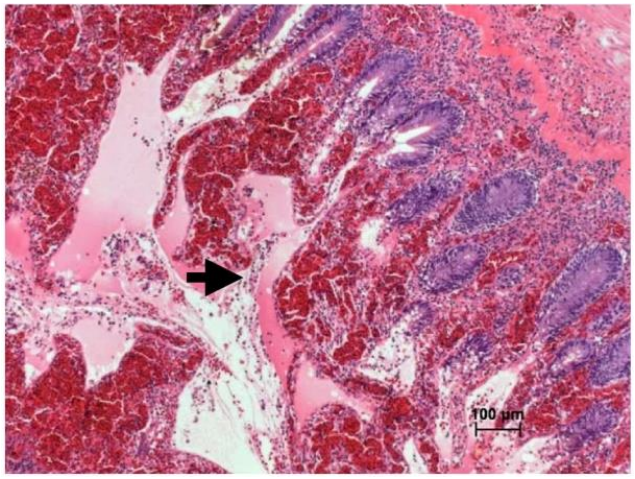

Figure 1.5b: An intestinal section of Atlantic salmon, the arrow indicates haemorrhages and ulceration of the intestinal mucosa. Adapted from Godoy et al., (2008).

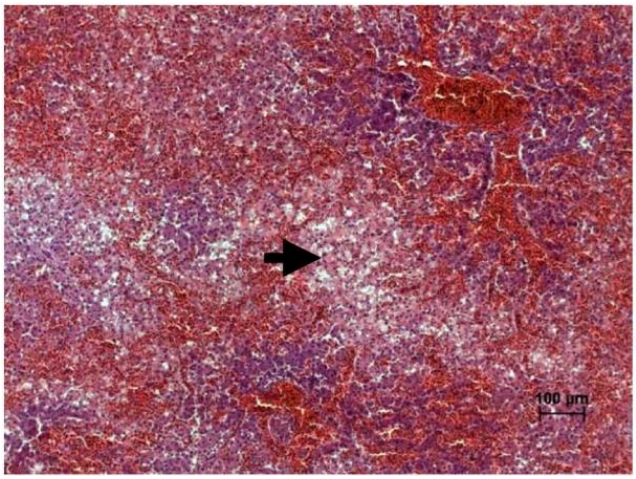

Figure 1.5c: A section of the liver from Atlantic salmon, the arrow indicates hepatocellular necrosis and sinusoidal peliosis along with haemorrhages. Adapted from Godoy et al., (2008).

1.5.1 Mortality rate and treatment options

Significant variation can be seen during an ISAV outbreak however rate of mortality may exceed 90% in severe cases. (B. H. Dannevig et al., 2008). Currently there is no completely effective vaccination or treatment options available in cases of ISAV infection (Gervais et al., 2021). According to OIE (2021), current available vaccines do not offer complete immunoprotection in affected individuals moreover inactivated whole virus vaccines do not provide clearance of viral load thereby rendering them as viral carriers**.** Chemotherapy, Immunostimulation, use of blocking agents and restocking with species that are resistant are also not applicable for control and prevention of ISAV (OIE, 2021). Limitations of treatment

options combined with high mortality rate renders ISAV outbreaks renders ISAV infections detrimental to aquaculture industry and Salmon farming, especially in Norway.

1.6 Cell lines for Infectious salmon anemia virus propagation

It is well established that cell lines can be used for studying salmonid pathogens along with host response and genetic engineering of cell lines show immense potential for the advancement of research in fish health (Collet et al., 2018). ISAV growth is supported by 5 cell lines(Rolland et al., 2005). CHSE-214 cell line 15 was found to be a suitable cell line for ISAV propagation along with Atlantic salmon (AS) cell line 20 but however, not all ISAV isolates seem to be supported by CHSE-24 and there is an absence of conspicuous CPE in the AS cell lines (Grant & Smail, 2003; Rolland et al., 2005). TO cell line is another cell line that supports ISAV growth however it is patented (Grant & Smail, 2003). ASK cell line is a cell line that was developed from the kidney tissues of Atlantic Salmon and is also highly sensitive displaying distinct CPE within 4 to 8 days of inoculation (Grant & Smail, 2003; Rolland et al., 2005). Similarly, SHK-1 cell line was established as a cell line by Dannveig et al., using the pronephros tissues of Atlantic salmon , can produces CPE and currently, is widely used for ISAV isolation and study (Rolland et al., 2005).

Thus, ASK cell line and SHK-1 cell line, both appear to be good choices as cell lines for ISAV propagation based on sensitivity and CPE effect. For our experiment, we followed the protocol of Virus quantification and propagation as per the work by Dannevig et al , the original developer of SHK-1 cell line and therefore for this particular experiment SHK-1 cell line was decided as the cell line for viral propagation and experimentation (B. H. Dannevig et al., 2008)

1.7 Similarities and differences between ISAV and Influenza virus

Influenza A, B, C, Isavirus and Thogotavirus comprise the five genera of *Orthomyxovirdae*. The genus of Thogotavirus includes Thogoto virus and Dhori virus whereas Isavirus genus consists of the ISAV. (Toennessen et al., 2009). As previously mentioned, both Infectious salmon anemia virus and Influenza Type A virus belong to the *Orthomyxoviridae* family, and Influenza type A virus is widely considered as a reference model for ISAV study (Cárdenas et al., 2022). ISAV is said to be an ‘evolutionary remote’ to influenza virus and it uses the similar mechanisms for cellular entry and exit as Influenza viruses (Toennessen et al., 2009). As discussed in section **1.4.2**, the 3’ end of genome segments of ISAV has 7 conserved

nucleotides whereas 5' end has 8 conserved nucleotides, comparatively shorter than the Influenza A virus and this has been suggested to contribute to the low replication temperature for ISAV in cold-water fish (Fourrier et al., 2014; Toennessen et al., 2009b).

In case of Influenza viruses, host cell attachment is mediated through the sialic acid binding domain on the viral fusion protein but however, in case of ISAV it encodes a Fusion protein which has neither receptor binding activity nor receptor destroying activity and it is HE protein that has that function (Cook et al., 2017; Müller et al., 2010). In case of ISAV the binding to 4-O Acetylated Sialic acid receptor does not induce a conformational change and hence is an unlikely trigger activate fusion protein for the fusion between host and viral membrane (Cook et al., 2017) whereas for influenza virus, the change of HA protein from non fusogenic structure to fusion active conformation on exposure to acidic pH of endosome regulates the membrane fusion between the viral and host membrane (Carr et al., 1997).

In case of Influenza-C virus, *N*-acetyl-9-O-acetylneuraminic acid is the preferred sialic acid receptor and the receptor destroying enzyme is acetyl esterase instead of neuraminidase and the HEF protein carries out all three functions of binding with sialic acid, esterase and membrane fusion activity whereas for Influenza A and Influenza B viruses, HA and NA proteins bind with sialic acid receptor and show neuraminidase activity (Matrosovich et al., 2013). In case of ISAV, both the sialic acid binding and acetyl esterase activity are carried out by HE protein unlike the HEF protein function in Influenza C virus (Matrosovich et al., 2013).

1.8 Candidate genes considered

The similarities and differences between ISAV and Influenza Type A have been discussed in the previous section. Compared to ISAV, higher amount of research has been carried out in understanding of the Influenza viruses. A genome wide CRISPR screen for host dependency factors for Influenza Type A infection was carried out by (Li et al., 2020). This work validated the host genes – *TMEM199, CCDC115* and *WDR7* as essential components for V-type ATPase assembly and for viral pathogenesis in host cell.

These three genes were essential for viral entry into the chosen cell in HA/NA dependant manner but did not influence the viral attachment to sialic acid receptors, which are the surface receptors for IVF-A virus (Li et al., 2020). The genes however played a non-negligible role in endosomal acidification and the loss of these genes resulted in endo-

lysosomal expansion and change in optimal pH gradient leading to coagulation of viral ribonucleoprotein (Li et al., 2020).

A work by B. Dannevig et al., (1995), involved inoculation of SHK-1 cells with ISAV particles in both presence and absence of substances that were associated with the inhibition of acidification in the cell organelles involved in endocytic pathways. Inhibitor of vacuolar ATPase like bafilomycin and weak bases like chloroquinone and ammonium chloride, all inhibited the CPE development compared to the control group thus indicating that ISAV infection in SHK-1 cell lines is low pH dependant and may be endocytic in nature (B. Dannevig et al., 1995; Pérez & Carrasco, 1993). Similarly, in a work by Eliassen et al., (2000) on SHK-1 cell line, when the cellular vacuolar pH was increased (made less acidic) using ammonium chloride or chloroquinone, there was endo-lysosomal accumulation of the ISAV and lowering of pH extracellularly resulted in increased ISAV production and at the same time, presence of chloroquinone in viral inoculation reduced the synthesis of ISAV, thus indicating that viral and host cellular membrane fusion occurs in endosomal acidic environment, thus further providing an evidence for similarity between ISAV and Influenza Type A virus (Eliassen et al., 2000). The gene *TMEM199* is a necessary component for endosomal acidification in cells (Miles et al., 2017). On literature review, we could not find sufficient works elucidating the role of these genes in ISAV pathogenesis. This prompted us to consider the role of the genes- *TMEM199*, *WDR7* and *CCDC115* in development of ISAV pathogenesis.

1.9 CRISPR as gene editing tool

CRISPR (Clustered Regularly Interspaced Short Palindromic Sequence) or the CRISPR-associated Cas System is a component on adaptive immunity in bacteria, the discovery of which has revolutionized genome engineering and has been successfully used for genome modifications in animals and plants(Sander & Joung, 2014) . CRISPR/Cas system is divided into two classes based on Cas proteins as Class 1 which includes Type 1,3 and 4; and Class 2 which includes type 2,5 and 6. The difference lies in Class1 consisting of Cas protein complexes made up of multi subunits whereas Class 2 consists of a single Cas protein (example: Cas 9) and is relatively simple and most widely studies.(Asmamaw & Zawdie, 2021).

The CRISPR cas9 technology involves two components, first one is a guide RNA to match the target gene sequence and an endonuclease (ex.: Cas 9) which can cause a double stranded DNA break (Redman et al., 2016).

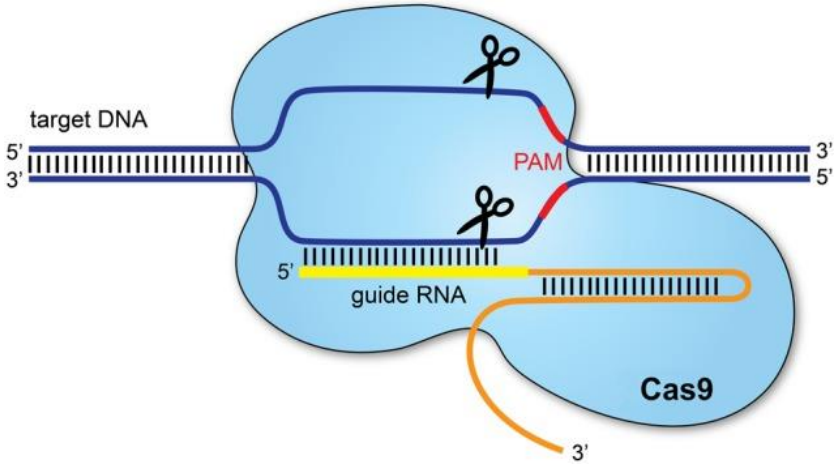

Figure 1.6: Figure representing the CRISPR/Cas9 system. Adapted from Redman et al., (2016).

The three steps of CRISPR can be summarized as recognition, cleavage, and repair.(Shao et al., 2016). As mentioned before, sgRNA (single guide RNA) and Cas9 nuclease are the two important components of a CRISPR/Cas9 system (Jinek et al., 2012).

The crRNA constitutes of a protospacer which is complementary to the target DNA sequence (Garneau et al., 2010). A formation of RNP (Ribonucleoprotein) complex occurs post hybridization of tracrRNA to crRNA and direct binding to the Cas9 protein.(Jinek et al., 2012). The cas9 protein has two lobes namely – nuclease lobe and a target recognition lobe. RuvC, HNH and PAM interacting domains constitute the three domains of nuclease lobe. A double stranded break of DNA ensues post cleavage of target DNA strand by HNH domain based on crRNA complementarity and other strand is cleaved by RuvC domain (Jinek et al., 2012, 2014).

A section of single guide RNA (which can be artificially synthesized- gRNA) binds to the genomic segment of DNA / target with the help of Cas9. (Redman et al., 2016)A proto spacer adjacent motif (PAM) must be present at 3'end of the gRNA in order to facilitate a cut. This is followed by repair which can be either non homologous end joining leading to A random deletion or insertion in segment , or by homologous end joining where repair template will utilize a homologous piece of DNA (Redman et al., 2016). Atlantic salmon genome has been successfully edited in-vivo using the CRISPR Cas9 technology (Edvardsen et al., 2014).

SHK-1 cell lines have been successfully edited using Crispr Cas9 technology (Gratacap, Jin, et al., 2020).

1.9.1 Delivery methods for CRISPR/Cas9

Several methods are available for the delivery of CRISPR cas9 components into the target cells. The methods may either be viral or non-viral in nature. Lenti viral transduction is a popular method of viral nature for CRISPR component delivery (Dong & Kantor, 2021). The non-viral physical methods involve delivery of plasmids or RNP complex of Crispr components, for example electroporation., however, off target effects, immunogenicity, insertional mutagenesis and targeted delivery are some of the challenges involved with the CRISPR delivery methods (Chandrasekaran et al., 2018)

Lentiviral transduction showed poor success rate in SHK-1 cell line, with less than 1% successful transduction of the cells (Gratacap, Regan, et al., 2020). Use of Cas RNP complexes and electroporation as a method of transfection is highly effective (more than 90% edit of SHK-1 cells), rapid and time effective compared to use of lentiviral vector/plasmids which are not only time consuming but also warrant promoter optimization and limitations for selection marker choices in fish cell lines due to little available information (Gratacap, Jin, et al., 2020)

1.10 Genome duplication in Atlantic salmon

Homology can be defined as a relationship characterized by a common descent in between two entities and thereby two genes that are homologous are called homologs (Koonin, 2005). Homologs can be sub classified as either orthologs or paralogs wherein orthologs refer to genes related through a speciation event of vertical descent and paralogs are essentially genes that are related via the event of duplication (Fitch, 1970; Koonin, 2005)

Whole genome duplication (WGD) can be described as a phenomenon characterized by doubling of the genome which tends to increase the genome complexity(Moriyama & Koshiba-Takeuchi, 2018). Around 80 million years ago, the common ancestors of salmonids underwent a whole genome duplication event (Ss4R) (Lien et al., 2016). All teleost members share a minimum of three events of whole genome duplications, with the first event (1R) and second event (2R) prior to divergence of lamprey from the group of Gnathostomata(Smith et al., 2013). The third whole genome duplication event (Ts3R) of teleosts occurred around 320 million years ago (Jaillon et al., 2004; Kasahara et al., 2007)

2 Aim

The primary aim of this experiment was to investigate if the genes - *WDR7*, *CCDC115* or *TMEM199* played a role in development of Infectious salmon anemia virus infection in SHK-1 cell line. To achieve this, we aimed at designing an effective guide RNAs for use in CRISPR/Cas9 knockout of SHK-1 cell line. Secondly, we aimed at quantitation of virus titre followed by a virus challenge study, in order to evaluate the effect of gene knockout.

3 Materials and methods

The three main sections of this experimental design can be summarized as – Identification of target genes, CRISPR/Cas9 based knockout of the target genes followed by the virus challenge of cell culture and analysis.

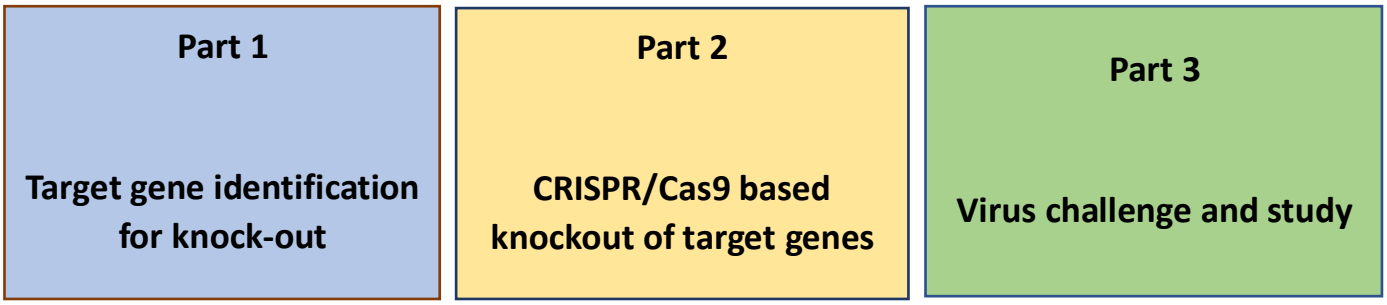

Figure 3.1: Schematic representation of the three main sections of this experimental design

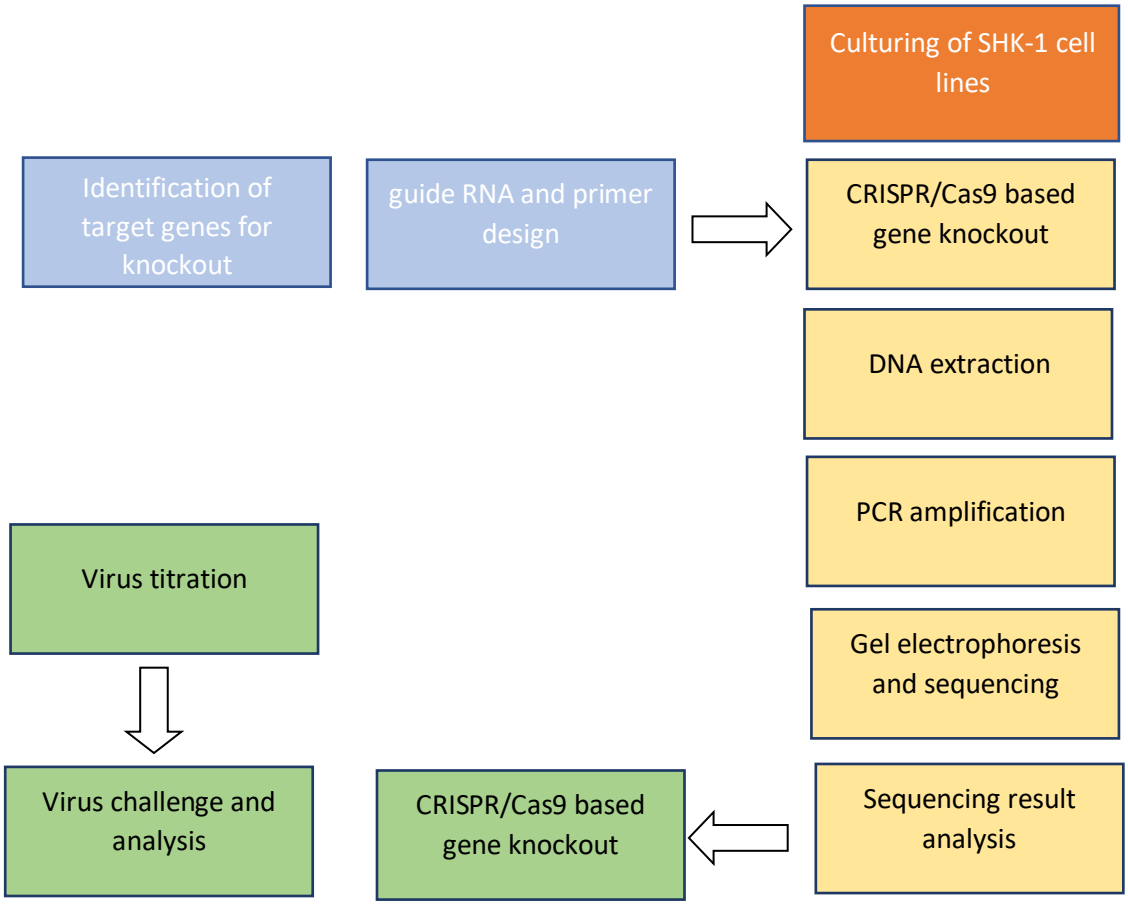

Figure 3.2: Flow diagram summary of the steps involved in the experiment

3.1 Cell culture

3.1.1 Cell line

Based on the information in section **1.6**, the cell lines chosen for this experiment was SHK-1 (Atlantic Salmon Head Kidney – 1) due to the effectiveness for Infectious salmon anemia virus propagation and appearance of distinct cytopathogenic effect (CPE) (B. Dannevig et al., 1995). The cell line was sourced from Øystein Evensen and Amr Ahmed Abdelrahim Gamil, Norwegian University of Life Sciences. The cell culture protocol was followed as per the instructions listed by the European Collection of Authenticated Cell Cultures (ECACC), along with certain modifications.

3.1.2 Cell culture protocol

Cell flask used for the cell culture was T75 (Thermo Scientific™ Nunclon™ Sphera™ Flasks) with a culture area of 75cm^2. Media composition was Leibovitz's L-15 + 10% Fetal Bovine Serum, Penicillin-Streptomycin 1% was chosen as the Antibiotic, 40µM 2-Mercaptoethanol (2ME). The cell cultures were incubated at a set temperature of 20°C.

Following a confluency of more than 75 % - 80%, the cells were sub-cultured into new T75 flasks depending on the cellular concentration with an aim of ensuring approximately around 2 million cells per new T75 flask.

Under the laminar flow hood, the old media was discarded, followed by washing of the flask with 3 ml of PBS (Phosphate Buffer Saline), twice and ensuring to swirl the flask before discarding PBS each time, so as the PBS covers the entirety of the base-flask surface area over the cellular attachment. This made sure that that most of the dead and unattached cells were washed away along with PBS. 3 ml of 0.05% Trypsin was then added into the flask and the flask was swirled to make sure that the Trypsin covers the whole base-flask surface area of attached cells. The next step involved waiting for the action of trypsinization that would result in the cells being unattached from the flask surface.

The flask was taken outside the laminar hood aseptically and the cells were monitored under microscope to see those changes. Morphologically, the cells appear to become rounded and free floating after the being trypsinized. It was observed that this complete process took an average of 20-25 minutes, with the aforementioned reagent concentration and quantities. Under the laminar flow hood, 3ml of fresh media was added to the flask to arrest further trypsinization and the whole fluid media from the flask was then transferred to a 50 ml falcon

tube. 10 µl was pipetted and used for cell counting and the remaining fluid media of suspended cells was centrifuged for 5 minutes.

For cell counting, 0.4% Trypan blue was used as the dye and the cell counter used was TC-20 Automated cell counter. Following centrifugation, there is a solid – liquid phase separation. Under the laminar flow hood, the liquid supernatant was then discarded, and the pellet was re-suspended in new media and redistributed into new T75 flasks, ensuring 10 ml of new media in each of the flaks. The cell growth was monitored every day and the flasks were washed using PBS every 3rd day or sooner in case of higher dead cell count and free-floating debris in media. As per the European Collection of Authenticated Cell Cultures (ECACC), use of conditioned media has been suggested during sub- culturing of the cells, however, following instances of bacterial contamination on use of conditioned media, it was decided to use a freshly prepared media entirely for every sub-culture; we observed less instances of contamination and cells showed no higher mortality rate compared to using conditioned media

3.2 Part 1 -Target gene Identification for knockout

Summary of Part 1

The primary step of this experiment was identifying the target genes involved with ISAV infection of cells for CRISPR/Cas9 based knockout. We considered 3 candidate genes as primary targets – *TMEM199, WDR7 and CCDC115*. This was followed by design of guide RNA and primers for the respective genes. The materials used and the steps followed for the same have been discussed in detail in the subsequent sections.

3.2.1 Phylogenetic study

The primary target genes under consideration were *TMEM199, WDR7* and *CCDC115*. Phylogenetic study for the above delineated genes was carried out using Salmobase (https://salmobase.org/). Salmobase is an integrated molecular data resource for the Salmonid species (Samy et al., 2017). We found that the gene *TMEM199* has been named *tm199* in NCBI, however the sequence remains the same and in the subsequent sections of the thesis, the name *TMEM199* has been used.

Primary target genes:

Table 3.1: Table indicating the Gene ID and gene name of the target genes in this experiment

Sr. number	Gene ID	Gene name
1	100286731 (NCBI)	*CCDC115*
2	106568530 (NCBI)	*WDR7*
3	100195903 (NCBI)	*tm199/ TMEM199*

Gene 100195903: *tm199*

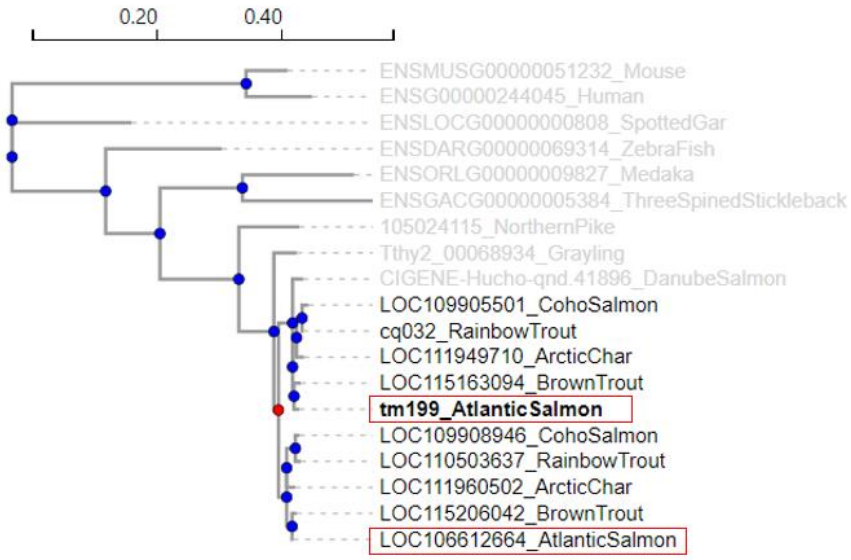

Figure 3.3: Figure showing the phylogenetic tree for the gene *tm199* in Atlantic Salmon.

Source: https://salmobase.org/genes/AtlanticSalmon/tm199

The gene duplications for the gene *tm199* have been placed inside a red box in the figure above.

Gene 106568530: *WDR7*

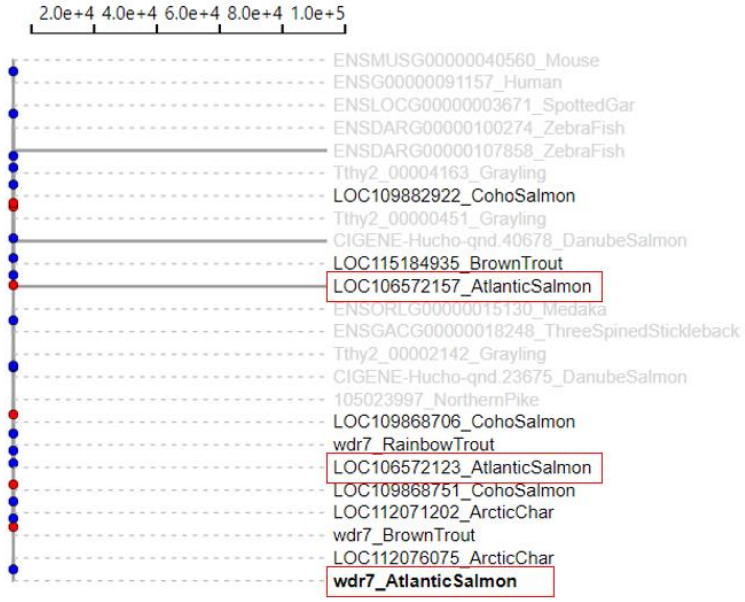

Figure 3.4: Figure showing the phylogenetic tree for the gene *WDR7* in Atlantic Salmon.

Source: https://salmobase.org/genes/AtlanticSalmon/wdr7

The gene duplications for the gene *WDR7* have been placed inside a red box in the figure above. However, the LOC106572157 was replaced with LOC106572123 in NCBI, as dated 11th January,2022.

Gene 100286731: *CCDC115*

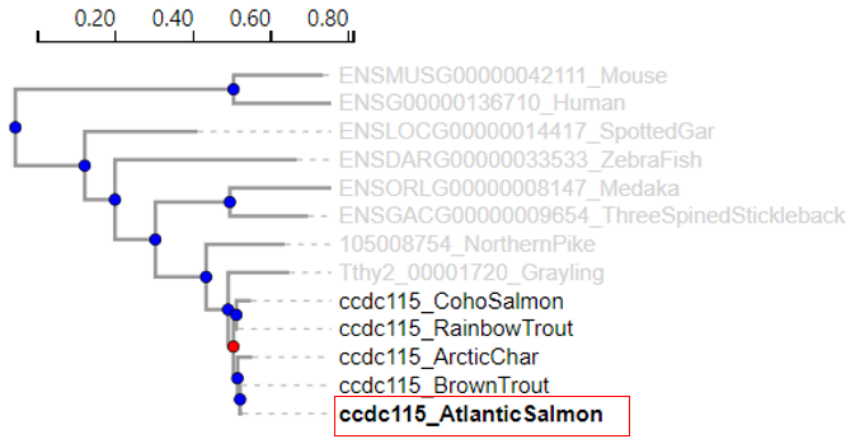

Figure 3.5: Figure showing the phylogenetic tree for the gene *CCDC115* in Atlantic Salmon.

Source: https://salmobase.org/genes/AtlanticSalmon/ccdc115

As we can see from the figure above, the gene *CCDC115* does not show any duplications in its phylogenetic tree.

The National Centre for Biotechnology Information webpage resource (https://www.ncbi.nlm.nih.gov/) was used to assemble complete gene information including Gene IDs and FASTA data for all the genes. The FASTA data (**7.3 Appendix**) for each gene was then imported into an alignment tool. The alignment tool used for this experiment was the software of Benchling (https://benchling.com/editor). The software of AliView (https://ormbunkar.se/aliview/), developed by Uppsala University, Sweden, was used as an alignment viewer tool to better understand the relationship between the gene duplications

3.2.2 Guide RNA and primer design

Guide RNA was designed using the gRNA design software of chopchop (https://chopchop.cbu.uib.no/). For the design of guide RNAs special emphasis was placed on location, GC content, complementarity, number of mismatch and the efficiency percentage. Suitable gRNAs that were thus chosen, were imported and aligned alongside their respective original gene sequence in Benchling (https://benchling.com/editor).

Primer design was carried out in Benchling (https://benchling.com/editor) using the 'Primer wizard' tool. Melting temperature was set at 58 ℃. As a positive control sample for the experiment, the guide RNA and primer for the gene *SLC45A2* was used, based on the work by Edvardsen et al (2014).

Table 3.2: Table enlisting the designed guide RNA, forward and reverse primers for the genes *WDR7*, *CCDC115* and *TMEM199*.

Sr. number	Gene name	No. of guide	Guide RNA	Forward Primer	Reverse primer
1	*WDR 7*	1	AGTGTGACGCC CGGGTCGGG	CATCGACTTCACAC GCTGACAG	CTCCATTAACCCC CTCACCTCC
		2	ACAAATCTTAC CTGTAAAGG	TTACTGAGTGTCGG CCGTTTTG	TGACAGGTGCCTT CTTCATATG
2	*CCD C115*	1	GTATTCGATGG GCAACAAGC	ACGGAAATGGTAT TTGAAGCCTCG	TCCAAACGCGGA TCACTTGTTC
		2	TCGTCGAACTG TGAGACGGT		
3	*TME M199*	1	GCTACAAGTAG AGAATGCTC	TAAGAGCATGGAC GACCAGGTC	CTTAGGCAGGTGC AATGAGCTG
		2	CAGAGCTGTAT GTTCTGGTA	ATTGGATTGACAC ATGGCAGCC	AGTTGGGAAACA CGGAGTCAAC

3.3 Part 2- CRISPR/Cas9 based knockout of target genes

Summary of Part 2

The second part of this experimental setup, post the identification of target genes and guide RNA- primer design, was the use of CRISPR/Cas9 molecular technology for knockout of the target genes. This section involves two sub- sections, the knockout experiment followed by the analysis of knockout. Some of the steps involved in the knockout experiment are - optimization of Cas9 and electroporation, preparation of Ribonucleoprotein (RNP) complex for electroporation, cell plating and electroporation. Whereas the analysis of knockout includes – extraction of DNA, Polymerase Chain reaction, agarose gel electrophoresis followed by sequencing. The two sub sections have been explained in detail below.

CRISPR/Cas9 based knockout experiment

Overview of steps involved in the knockout experiment are:

- Optimization of Cas 9 concentration
- Optimization of electroporation – pulse, voltage and time
- RNP preparation
- Cell plating
- Electroporation

3.3.1 Cas 9 optimization

Prior to knockout experiment, optimization of Cas9 concentration for CRISPR knockout was performed. This enabled us to determine the Cas9 concentration that resulted in relatively higher knockout score post sequencing, based in our laboratory setting. This was based on drawing references from the work by Gratacap, Jin et al., (2020). Ribonucleoprotein (RNP) complex with following Cas 9 concentration was set up. The target gene was *SLC45A2*. The RNP preparation step has been explained in the section **3.3.3**. The knockout protocol in Sandvik group was followed based on the work by Edvardsen et al. (2014).

Table 3.3: Table with the RNP complex and media concentration against the respective Cas9 concentration

Serial Number	**Cas 9 Concentration (µM)**	**RNP (µM)**	**Media (µl)**
1	0.35	0.42	11.58
2	0.70	0.84	11.16
3	1.05	1.26	10.74
4	1.40	1.68	10.32
5	1.75	2.10	9.90
	Total	6.30	53.70

Post Ribonucleoprotein (RNP) preparation, electroporation, PCR and sequencing of the samples, analysis of knockout score was performed using the ICE Synthego software

(www.synthego.com/products/bioinformatics/crispr-analysis). The steps associated with all the protocols from sample preparation to analysis, was similar as the main experiment and has been explained in further detail in subsequent sections. Post sequence analysis, a second round of similar experimental set up was then performed using the concentration of 1.75 µM (explained in further detail in section **4.1.1**) and higher to further analyse the possibility of higher concentration corresponding to higher efficiency.

Table 3.4: Table showing the RNP complex and media concentration against the respective Cas 9 concentration

Serial Number	**Cas 9 Concentration (µM)**	**RNP (µM)**	**Media (µl)**
1	1.75	2.10	9.9
2	3.5	4.2	7.8
3	7	8.4	3.6
4	10	12	0
	Total	26.7	21.4

Post sequencing, analysis, Cas 9 concentration of 7 µM was chosen as the optimized concentration for this particular knockout experiment (section **4.1.1**).

3.3.2 Optimization of electroporation

Post Cas9 optimization, next step involved optimization of electroporation protocol for pulse, voltage and time. This was based on the protocol for gene *SLC45A2* (Edvardsen et al., 2014) and also drawing reference from the work by (Gratacap, Jin, et al., 2020) and previous experiments performed in Sandvik group. The parameters mentioned in the table below, was hence chosen as the optimized electroporation protocol for this particular experiment.

Table 3.5: Table showing the optimized electroporation voltage, pulse and time.

Voltage	Pulse	Time
1600	3	10 minutes

3.3.3 Ribonucleoprotein (RNP) preparation

Ribonucleoprotein (RNP) complex comprises of Cas9 protein and gRNA (crRNA and tracrRNA) as an effective delivery medium for CRISPR/Cas9 based knockout (Zhang et al., 2021). 1µl cRNA was added to 1µl tracrRNA (100µM), mixed together using pipette and annealed in PCR using a temperature of 95 ℃ for a period of 5 minutes and then cooled down slowly to room temperature. The respective gRNAs were mixed separately and twice the volume of 20µM Cas9 was added. Number of replicates per gene was 4. This RNP complex was then incubated at room temperature for 15 minutes and then kept on ice until further use.

3.3.4 Cell plating

A 24 well plate (Nunc™ Cell-Culture Treated Multidishes, Thermo Scientific™) was used along with 1 ml of freshly prepared SHK-1 media as discussed in section (**section 3.1.2**) - without the antibiotic, was added in each well. The cells from the flasks (passage number 8) were washed with PBS, trypsinized and centrifuged. The steps for culture remain same until the step of centrifugation. Approximately 20000 cells were seeded per well and approximately, a total of 4.8 million cells were needed for a 24 well plate. Post centrifugation, the supernatant was discarded, and then further PBS (Phosphate Buffered Saline) was added and centrifuged again. The supernatant was discarded once again post centrifugation. This was followed by resuspension of cells in OptiMEM media to achieve a cellular concentration of 10^7 cells/ml.

Five Eppendorf tubes were labelled and 40µL SHK-1 suspension and 16µL of RNP associated with the respective genes were added to four of the tubes whereas the fifth tube without any RNP, was used as the negative control.

3.3.5 Electroporation and layout of wells

The Invitrogen™ Neon™ Transfection System kit was used for the purpose of electroporation. The protocol followed was as per instructions mentioned in the NEON (Invitrogen™) manual. The following voltage, pulse and time setting was followed based on the optimization protocol as discussed in section **3.3.2**.

Table 3.6: Electroporation voltage, pulse and time followed for the main experimental set up

Voltage	Pulse	Time
1600	3	10 minutes

For each gene, four replicates were electroporated from each of the tube, including the negative control. All of the samples were electroporated separately to avoid cross contamination. The electroporated samples were seeded into the 24 well plate in the following manner –

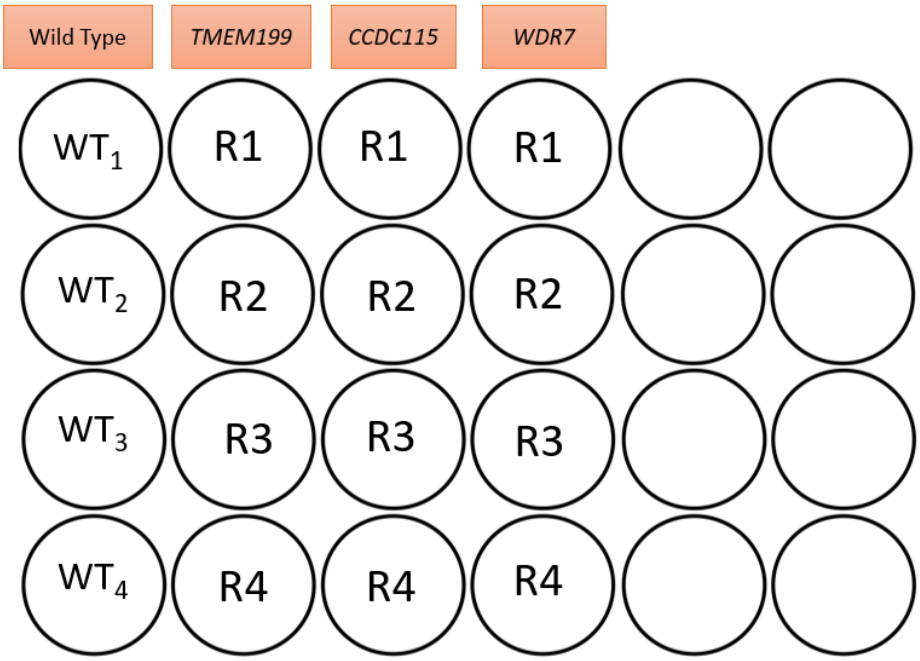

Figure 3.6: Image showing the experimental layout for electroporation. 'R' indicates replicate number for the particular gene sample.

The cell media was changed post 24 hour and 1 ml of fresh media containing the antibiotic (**section 3.1.2**) was added to each well. The cells were incubated until confluent.

Analysis of knockout

Overview of steps involved in the knockout analysis are:

- DNA extraction
- PCR
- Gel electrophoresis
- Sequencing

3.3.6 DNA extraction

Post electroporation of the cells in 24 well plates, the plates were monitored closely every day and observed for confluency. Post a confluency of approximately 80%, the media was pipetted out from all the wells and each well was washed with PBS twice. QuickXtract DNA kit was used for DNA extraction. Post washing, 0.5 ml of QuickXtract DNA was added to each of the respective wells. Post 5 minutes of incubation at room temperature, the wells were scraped gently using the pipette tip with a view of separating all the attached cells. All the cells were then collected in separate PCR tubes as per their well number and heated up to 65 °C for 15 minutes, and to 98 ℃ for 2 minutes in PCR machine.

3.3.7 Measurement of DNA sample concentration

The extracted DNA product was then loaded into separate tubes and labelled as per their respective gene and replicate wells. Samples were then loaded to Nanodrop spectrophotometer and DNA concentration in each well was measured. Table values indicating the specific DNA concentration of each sample has been attached in appendix IV. Concentration of the samples as measured by Nanodrop has been attached as a table in Appendix **7.3**, table **7.3.1**.

3.3.8 PCR protocol

The Polymerase Chain reaction was performed using the Platinum II Hot-Start Green PCR Master Mix kit (Thermofisher, 2018). The protocol involved 35 cycle denaturation.

Table 3.7: Temperature settings followed as per the Thermofisher manual for Platinum II Hot-Start Green PCR Master Mix kit.

Sr. No.	Step	Temperature	Time
1.	Initial Denaturation	94 ℃	2 minutes
2	Denaturation	94 ℃	15 seconds
3	Annealing	60 ℃	15 seconds
4	Extension	68 ℃	15 seconds/kb
5	Hold	4 ℃	Hold

The total reaction volume for each sample was 20µl. This included the extracted DNA sample, corresponding primer, nuclease free water, 0,4µl of forward and reverse primer (10µM concentration), 10µl PlatinumTM II Hot-Start Green PCR Master Mix (2x), and 4µl PlatinumTM GC Enhancer. The amount of template DNA used was along the range of 1-6 µl depending on the DNA concentration that was measured using the Nanodrop, so as to not exceed the concentration of 500 ng/rxn as per Thermofisher protocol for the PCR kit.

The amount of nuclease free water added to the DNA sample depended on the DNA concentration, as measured in Nanodrop. The relationship between the DNA concentration and the amount of nuclease free water used, is inversely proportional to each other. That is, higher the DNA concentration, lesser the nuclease free water added to the sample.

3.3.9 Gel electrophoresis

Gel electrophoresis and subsequent imaging was performed to evaluate to functionality of the primers. Gel run was performed using the standard agarose gel electrophoresis protocol. The concentration of agarose powder used was 1% along with TAE buffer (Tris-acetate-Ethylenediaminetetraacetic acid). In order to visualize the DNA bands under the imaging software, RedSafe™ Nucleic Acid Staining Solution (20,000x) was used. The size of gel ruler

used was 1kb ladder and the samples were run at 90V for approximately 35 minutes. Imaging was performed using the ChemiDoc XRS+ Gel Imaging System and the Image Lab 6.0 software.

3.3.10 Sequencing

The sequencing service of Eurofins genomics was used for this experiment and hence the protocol followed was as per Eurofins genomics. Certain modifications were made as per the protocols of Sandvik group. ExoSAP-ITTM Express PCR Product Cleanup reagent was used (Applied biosystems, 2017). The reagent sample being used was diluted to $1/10^{th}$ the concentration using nuclease free water. 1µL PCR product was mixed with 4µL ExoSAP-ITTM Express reagent. PCR incubation involved 37°C for 15 minutes, followed by 80°C for 15 minutes and then cooled to 4°C and kept on ice until further use. The DNA samples were then combined with a volume of 5µL (concentration of 5 pmol/µL) of the respective forward primer. The sample tubes were then labelled using the LightRun barcode stickers from GATC and were delivered at the delivery point for collection. The sample layout for the respective genes with their sample IDs have been included in the Appendix **7.3**, tables **7.3.2, 7.3.3** and **7.3.4**.

3.4 Part 3- Virus challenge and study

Summary of Part 3

This part of the experiment involves two sub sections. First sub section involves Viral titration. This step involves using the cell scoring method post appearance of virus induced CPE (B. Dannevig et al., 1995) followed by calculation of $TCID_{50}$/ml , FFU/ml (Focus Forming Units) and MOI (Multiplicity of Infection). Whereas the second sub section involves challenging of target gene knockout cell culture with ISAV in order to study the CPE.

Virus titration

Overview of steps involved in Virus titration are:

- Cell scoring post appearance of CPE
- Calculation of $TCID_{50}$/ml, FFU/ml and MOI

The virus culture protocol was followed as per the work done by B. Dannevig et al., (1995), along with minor alterations. The virus media consisted of L-15 media along with 1% by volume F.B.S., 40µM of 2 Mercapto Ethanol and the anti-biotic used was 1% Pennicilin-streptomycin (Pen.Strep). The virus solution from the vial was transferred to T75 flasks with SHK cells (approximately 80-90% confluent). The flasks were incubated at 15°C and observed regularly on day 5, day 7 and every day thereafter for monitoring the CPE. Post day 18, maximum cell death was observed in the flasks. On day 19, the media from the flasks were collected and then filtered (0.2 µm pore size) using 50 ml syringe.

Filtered media was then distributed into Eppendorf tubes (1 ml). One vial was used to infect a fresh batch of cell in t75 and kept in the incubator, this ensured a fresh batch of virus available for the laboratory use, as and when needed. Rest of the vials were stored in -80°C for further use of this experiment (E.S. Munro et al., 2007). According to the protocol by B. Dannevig et al., (1995), virus titration was performed to determine the appropriate virus dosage needed for infecting the cells. The primary principle is based on effective concentration and infective strength post serial dilution of the original viral stock concentration and calculation of $TCID_{50}$/ml, FFU/ml (Focus Forming Units) and MOI (Multiplicity of Infection).

3.4.1 ISAV titration

Approximately 10000 SHK-1 cells (passage number 9) were seeded into 64 wells (8x8) of the 94 well plate.

The layout of cells along with the virus distribution in terms of relative concentration has been described as a schematic in the image given below.

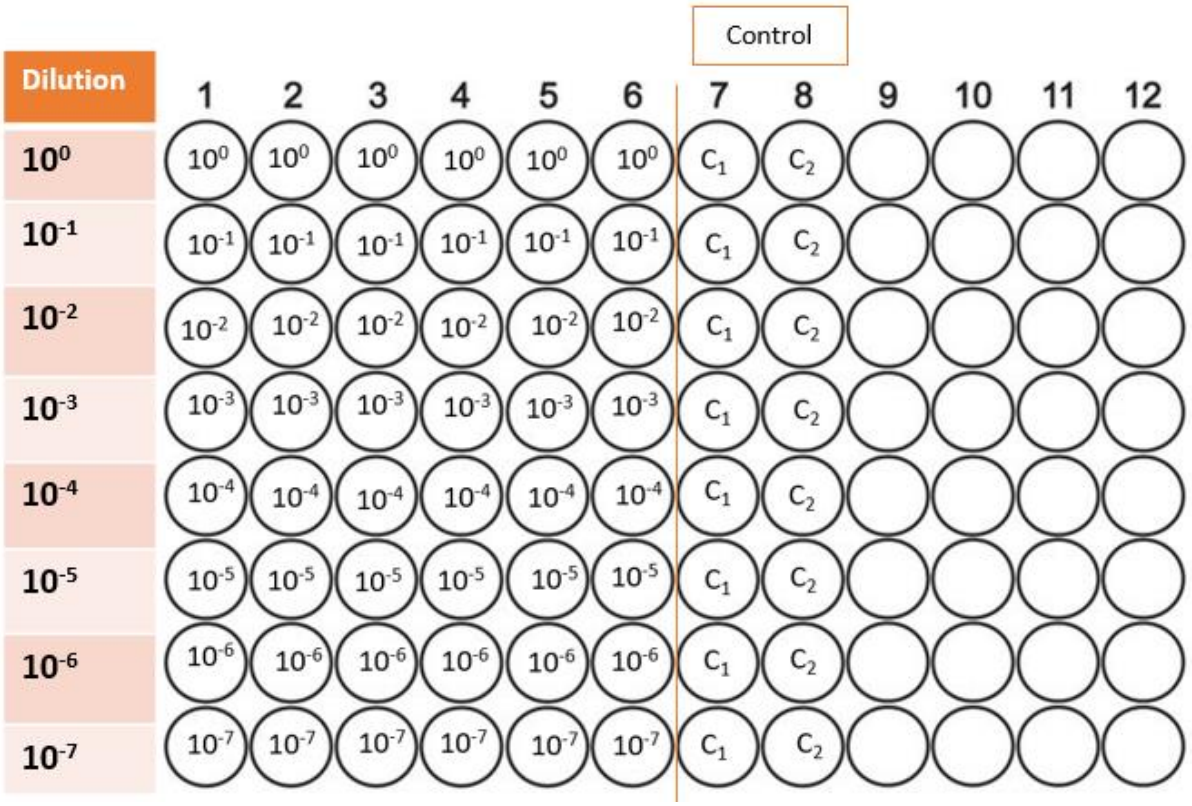

Figure 3.8: Layout of wells used for infection along with distribution of respective virus concentrations in terms of serial dilution. 10^0 indicates the original concentration of virus used without any dilution whereas 10^{-7} indicates $1/10^7$ times or 7 times dilution compared to the original concentration. Virus challenge with respective serial dilution was carried out from well number 1 up to well number 6. C1 and C2 i.e., well number 7 and well number 8, indicate the two control groups without any virus challenge and infection.

The original SHK –1 cell culture media was used. Approximately 300 µl of media was used in each well. Cells were observed every day for confluency. Confluency was observed approximately in 6-7 days and then the original media was discarded, and the wells were washed twice with PBS in order to remove the dead cells and other cellular debris. Then a fresh batch of virus media around 300µl (L-15 media along with 1% by volume F.B.S., 40µM of 2 Mercapto Ethanol and 1% Penicillin-streptomycin (Pen. Strep) was then pipetted into each well. Post confluency, 100 µl of virus inoculum from the frozen vial was used to challenge the cells in each well.

The plates were observed on day 5, day 7 and everyday thereafter until day 15. Cell scoring was performed on day 14 p.i. (post infection) as per the description by B. Dannevig et al. (1995), using EVOS ™ XL Core Imaging system (ThermoFisher Scientific) microscope. A positive score (+) was attributed to the wells showing more than 50% of CPE which is characterized by increased vacuolation, cell death and loss of cellular adherence (B. Dannevig et al., 1995). Post scoring, the information was used to calculate $TCID_{50}$. $TCID_{50}$ or the 50% Tissue Culture Infectious Dose is a commonly used measure of the dilution of a virus required to infect 50% of a cell culture (Lei et al., 2020). $TCID_{50}$was calculated using $TCID_{50}$ calculator by Department for Infectious Diseases , Molecular Virology – University of Heidelberg, Germany; based on the work by (Hierholzer & Killington, 1996).

3.4.2 ISAV challenge

Based on the results of virus quantitation, as discussed in section **4.3.2**, and the knockout efficiency analysis of primary target genes, a virus challenge setup for the genes *TMEM199, WDR7* and *CCDC115* was set up.

All the protocols of cell seeding, and virus challenge remained the same as per section **3.1.2** and section **3.5.2**, except that for the virus challenge experiment, gRNA was chosen based on sequencing results in section **4.2**. Guide number 1 (table **3.2**) was used for electroporation for the gene *tm199* and guide number 1 (table **3.2**) was used for the gene *WDR7*. Approximately 10000 cells (passage number 9) were seeded per well of the 96 well plate and 300 µl of SHK-1 virus media was used per well. Three experimental groups were set up namely – knockout infected group, control group and non-knockout infected group. The knockout infected group consisted of cells with respective gene knockout and then challenged with ISAV. Control

group did not receive any treatment. The non-knockout infected group consisted of cells without any gene editing, but they received ISAV challenge. A 2x12 layout with 4 replicates for each experimental group was used for this setup. 100 µl of virus was used in each well in order to ensure an MOI of 1.029. Frozen virus from the 1 ml vials stored in -80°C was kept on ice and thawed before being used for the experiment. Cell scoring was performed on day 14 p.i. (post infection) of SHK-1 cells, using EVOS ™ XL Core Imaging system (ThermoFisher Scientific) microscope.

A 96 well plate was used for this experiment, involving three wells for virus challenge of samples with respective knockout gene, as three replicates - R_1, R_2, R_3 and R_4. Control group consisted of non-knockout non-infected cells and the final group consisted of non-knockout cell group challenged with ISAV, as discussed before.

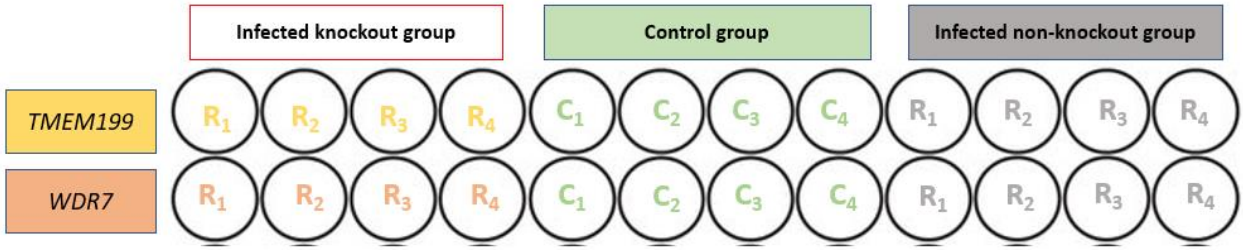

Figure 3.9: Layout of wells used for the virus challenge experiment. 'R' indicates the replicate number for the particular gene in the experimental group. 'C' indicates the replicate number for control group,

4 Results

4.1 Section 1 – Pre-sequencing

4.1.1 Optimization of Cas9 concentration

The method of Cas9 optimization has been discussed in section **3.3** under Materials and Methods. Two rounds of experiments were performed using *SLC45A2* as the target gene, in order to assess the knockout efficiency associated with Cas9 concentration. The first round of experiment was performed with a Cas9 concentrations of 0.35 µM, 0.70 µM, 1.05 µM, 1.40 µM and 1.75 µM (refer table **3.3**), highest editing efficiency of 63% was obtained for a Cas9 concentration of 1.75 µM.

A second-round d of experiment was performed in order to further analyse the efficiency on increasing the Cas9 concentration. Concentrations of 1.75 µM, 3.5 µM, 7 µM and 10 µM (refer table **3.4**), was analysed for editing efficiency and the Cas9 concentration of 7 µM yielded the highest knockout percentage at 53%. Hence, this was chosen as the Cas9 concentration for this experiment. Steps involved in analysis remained same as in section **3.3**. and post sequence analysis was performed using ICE SYNTHEGO CRISPR Analysis tool.

4.1.2 Gel electrophoresis

Post primer design, gel electrophoresis was performed to assess the functionality of the primers. The details of materials used for the primer design has been explained in the materials and methods section. (Insert detail about approximate band size in bp for each primer). We allotted four replicates of DNA for each corresponding primer pair along with one positive control and one negative control. Well number 28 and 29 was positive and negative controls, respectively. The positive control consisted of the primer for a previously established primer for the gene *SLC45A2*.

A trend of variability was seen amongst the band intensities for the samples. Some of the bands showed high intensity and some showed very low intensity. There were wells which also showed no bands.

Low or faint band intensity was consistent with the samples that had lower DNA concentration when measured in the Nanodrop. Some of the wells, inspite having a high DNA concentration showed faint or no bands, this implies an error in primer design, contamination, PCR optimization or technical factors like pipetting techniques, error during addition of reagents, improper temperature setting in incubation steps, faulty mixing of sample during the use of vortex machine etc. For the replicate samples, one showing high intensity band and other one showing low intensity band, faulty primer design is an unlikely cause. Interpretation and further discussion of the gel run can be found in section **5.2.2**.

For this experiment, several gel runs were performed in order to assess primer functionality. For the genes *WDR7, CCDC115* and *TMEM199*; samples showed a trend of variability in terms of band intensity. Gel runs were performed separately and ensured that bands were visible for all samples for the genes *WDR7, CCDC115* and *TMEM199* before treating and sending the post PCR product for sequencing.

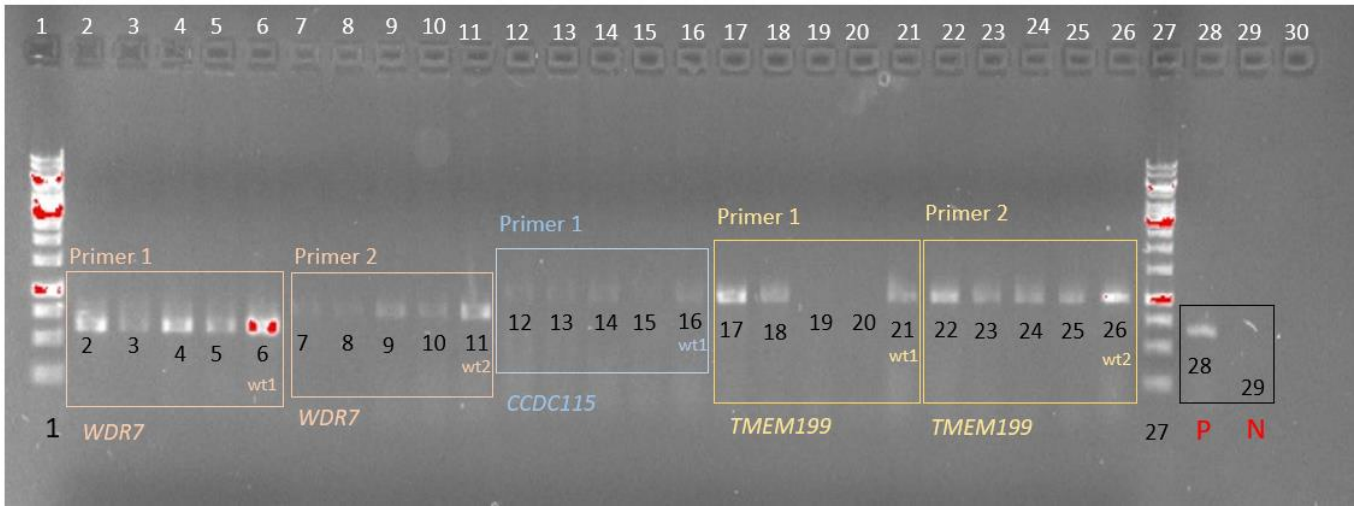

Figure 4.1: Figure visualizing the bands for genes *WDR7, CCDC115* and *TMEM199*, post Agarose Gel electrophoresis using ChemiDoc XRS+ Gel Imaging System and the Image Lab 6.0 software.

In the above image, wells have been numbered similar to the bands. Well number 1 and well number 27 are 1 kb ladders. All bands are in the range of approximately 500 – 1000 base pairs, consistent with their sequence length. Well number 28 is the positive control whereas well 30 is the negative control. Interpretation of the gel has been discussed in detail in section **5.1.2**.

4.2 Section 2- Analysis of genomic data post sequencing

4.2.1 Gene 100195903: *tm199* or *TMEM199*

The gene *TMEM199* had two set of guide RNAs along with their respective primer pair (forward and reverse) (table **3.2**). Each set of guide RNA had 4 replicates and one control sample (wild type). The layout which has been explained in table **7.3.2**.

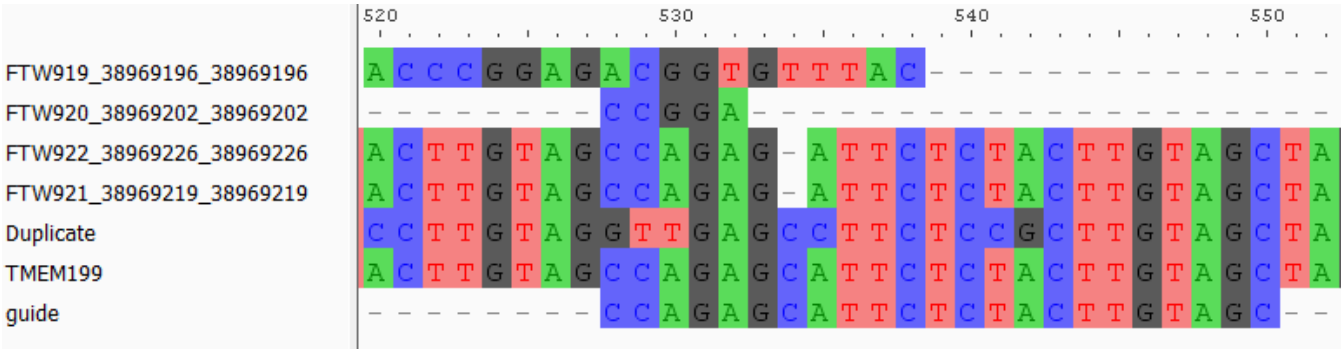

Figure 4.2: Image from alignment viewer tool AliView, showing the alignment of the corresponding DNA segment of guide RNA against the segment of gene *TMEM199*, duplicate gene and the analysed samples.

ICE CRISPR Analysis tool by Synthego was used to analyse the knockout score for the samples. We were able to achieve a knockout score of 98% for the gene *TMEM199*.

Figure 4.2.1: Relative contribution of each sequence for one of the replicate samples. The contributions show the inferred sequences present in the edited population and their relative proportions. Cut sites are represented by the black vertical dotted lines and '+' sign on left side of the image indicates the wild type. Source: ICE CRISPR Analysis tool by SYNTHEGO

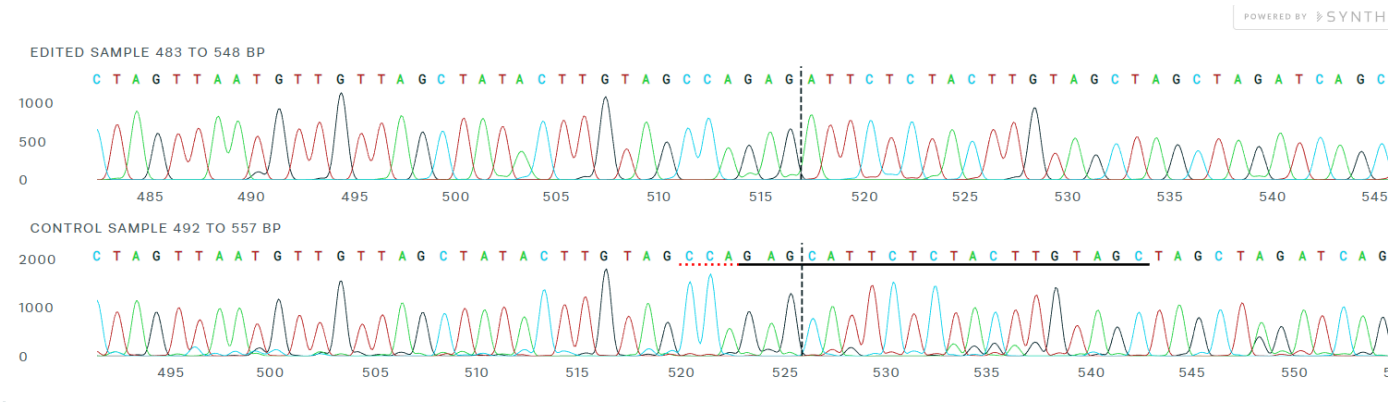

Image 4.2.2: This image shows the Sanger sequence view for the edited and the control (wild type) sequence in the region around the guide sequence. The horizontal black line represents the guide sequence whereas the horizontal red line is the PAM site. Vertical dotted black line represents the actual cut site. Source: ICE CRISPR Analysis tool by SYNTHEGO

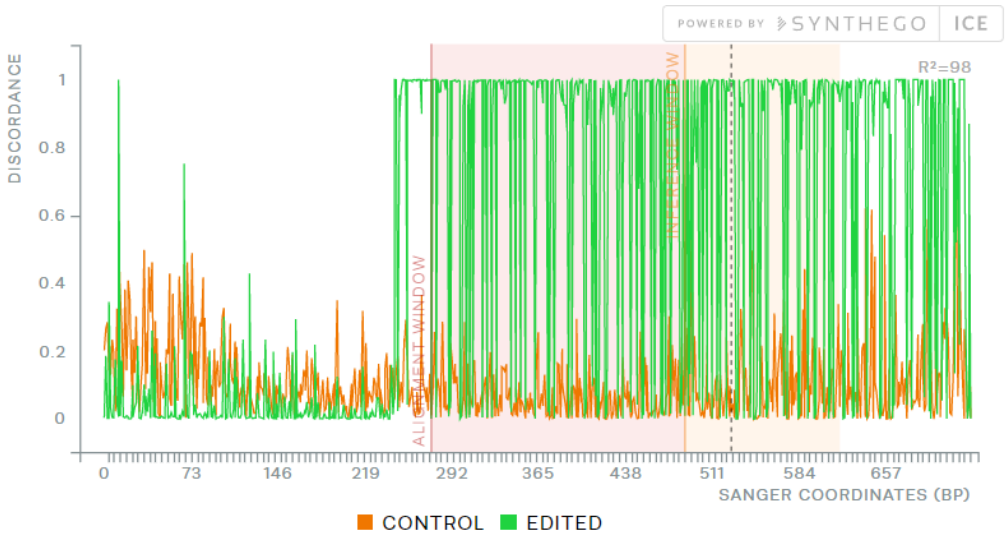

Image 4.2.3: This image shows the discordance plot for samples of the gene *TMEM199*. The plot details the level of alignment per base between the wild type and the edited sample in the inference window (region around the cut site) i.e., it shows the average amount of signal that disagrees with the reference sequence derived from the control trace file. On the plot, the green line and orange line and orange line should be close together before the cut site, with a typical CRISPR edit resulting in a jump in discordance near the cut-site and continuing to remain far apart after the cut site (representing a high level of sequence discordance). Source: ICE CRISPR Analysis tool by SYNTHEGO

4.2.2 Gene 106565198: *WDR7*

The gene *WDR7* had two set of guide RNAs along with their respective primer pair (forward and reverse) (Table **3.2**). Each set of guide RNA had 4 replicates and one control sample (wild type), just like the gene *TMEM199*. The layout which has been explained in table **7.3.3**. ICE CRISPR Analysis tool by Synthego showed a comparatively low knockout score of 6.

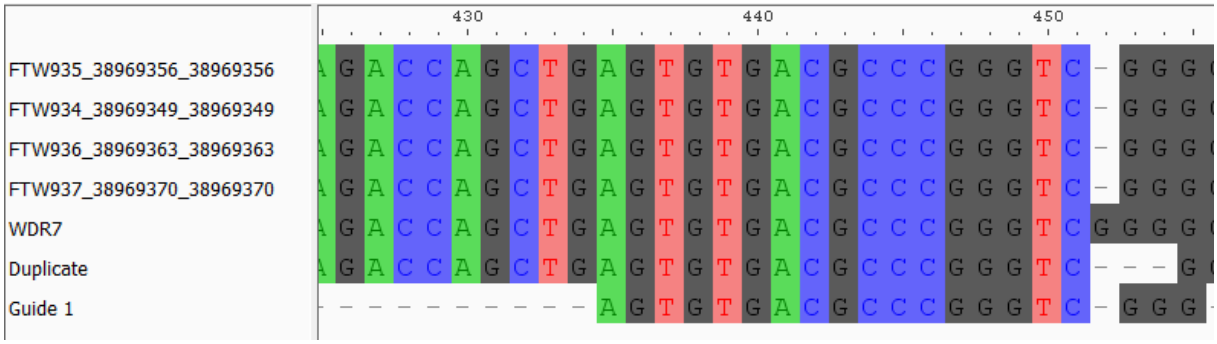

Figure 4.3: Image from alignment viewer tool AliView, showing the alignment of the corresponding DNA segment of guide RNA against the segment of gene *WDR7*, duplicate gene and the analysed samples

Figure 4.3.1: Image showing the relative contribution of each sequence for one of the replicate samples. The contributions show the inferred sequences present in the edited population and their relative proportions. Cut sites are represented by the black vertical dotted lines and '+' sign on left side of the image indicates the wild type. Source: ICE CRISPR Analysis tool by SYNTHEGO

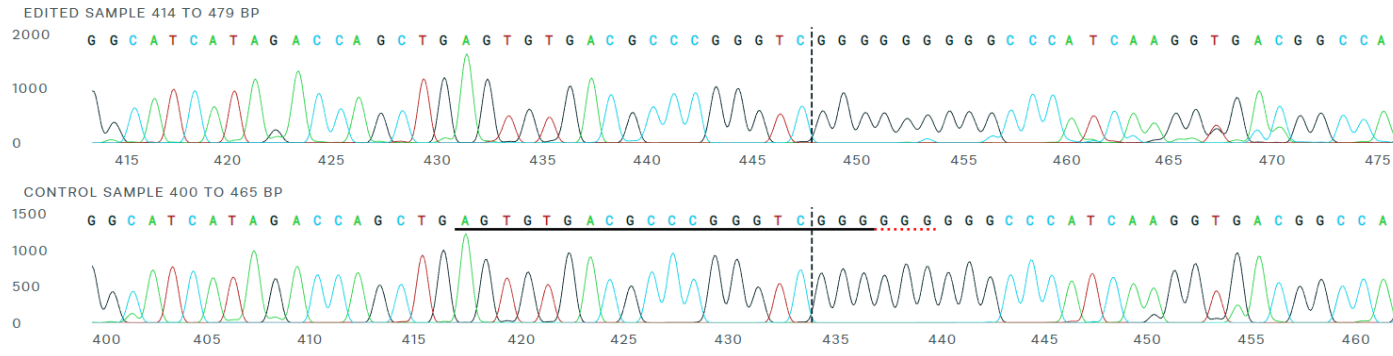

Figure 4.3.2: This image shows the Sanger sequence view for the edited and the control (wild type) sequence in the region around the guide sequence. The horizontal black line represents the guide sequence whereas the horizontal red line is the PAM site. Vertical dotted black line represents the actual cut site. Source: ICE CRISPR Analysis tool by SYNTHEGO

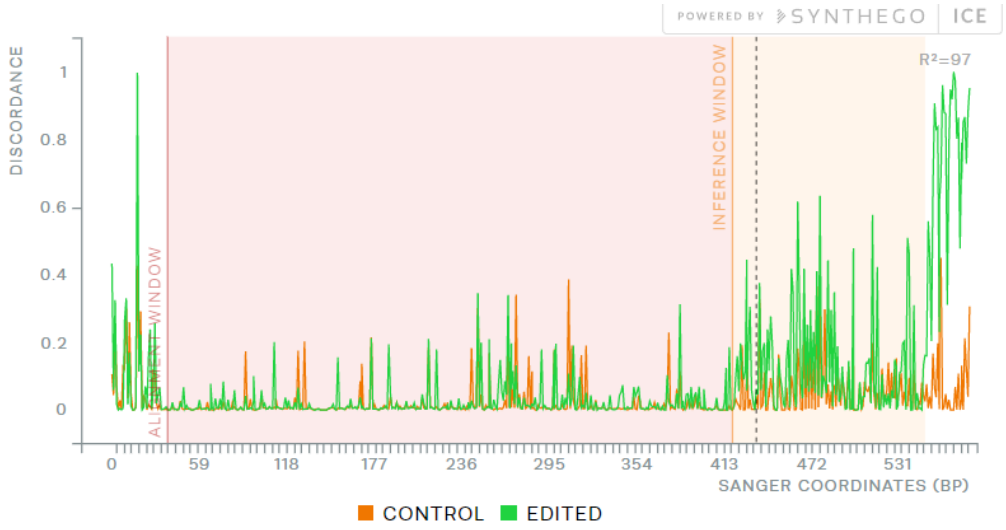

Figure 4.3.3: This image shows the discordance plot for samples of the gene *WDR7*. The plot details the level of alignment per base between the wild type and the edited sample in the inference window (region around the cut site) i.e., it shows the average amount of signal that disagrees with the reference sequence derived from the control trace file. On the plot, the green line and orange line and orange line should be close together before the cut site, with a typical CRISPR edit resulting in a jump in discordance near the cut-site and continuing to remain far apart after the cut site (representing a high level of sequence discordance. Source: ICE CRISPR Analysis tool by SYNTHEGO

4.2.3 Gene 100286731: *CCDC115*

In case of the Gene CCDC115, we can see that the samples (**7.3.3**) had a low-quality score and could not be sequenced and subsequently could not be analysed.

Figure 4.4: Image showing the low-quality score of samples. Source: ICE CRISPR Analysis tool by SYNTHEGO

4.3 Section 3- Virus titration and CPE study post ISAV challenge

4.3.1 Virus titration

As a part of the titration experiment, three separate batches of virus titrations were performed. Post virus challenge, CPE observation and cell scoring for one batch, the same process was repeated for the subsequent batches. The protocol for virus titration has been explained in section **3.4.1**.

The scoring of cells for virus induced cytopathogenic effect (CPE) in the cell line was performed as per the protocol by B. Dannveig et al., (1995). Consistent with the work by B. Dannveig et al., (1995) and OIE (2021), we observed a prominent and discernible CPE around day 13. The plates were observed on day 5, day 7 and subsequently every day until day 15. Cell scoring was performed on day 14 (p.i.).

Each well was observed carefully to observe parameters like confluency, live cells, adherence to well surface, mortality and cytopathogenic effect. Subsequently cells showing a mortality and virus induced cytopathogenic effect of more than 50% were scored with '+'. Cytopathogenic effect was characterized by loss of adherence and presence of cytoplasmic vacuolation (B. Dannevig et al., 1995). Cells without noticeable CPE (>50% were marke6d with '-'.

The results from the scoring were plotted into a $TCID_{50}$ calculator provided by Department of Infectious Diseases- Molecular Virology, University of Heidelberg, based on the Spearman–Kärber algorithm (Mahy & Kangro, 1996) as described in (Hierholzer & Killington, 1996). Subsequently FFU/ml (section **4.3.2**) and MOI was calculated based on principles by (Lei et al., 2020; Payne, 2017).

The layout of the experiment with the scoring result can be visualized in the image below -

Batch 1:

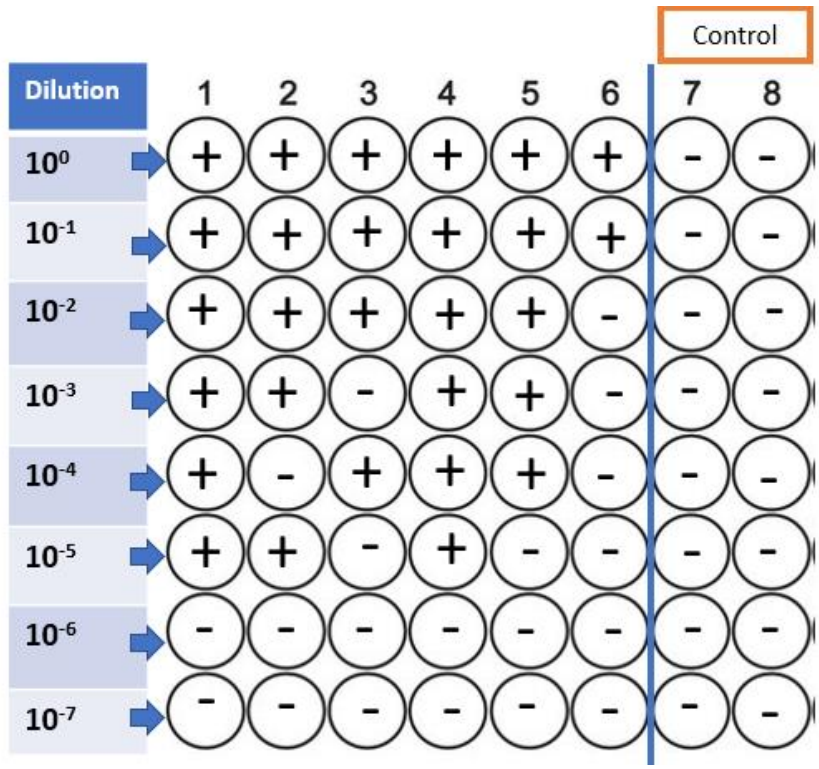

Figure 4.5.1: Figure indicating the layout overview for 1st batch of viral titration, with cell scoring performed on day 14 post infection. '+' indicates approximately more than 50% of CPE associated cellular mortality. '-' indicates absence of CPE associated cell death.

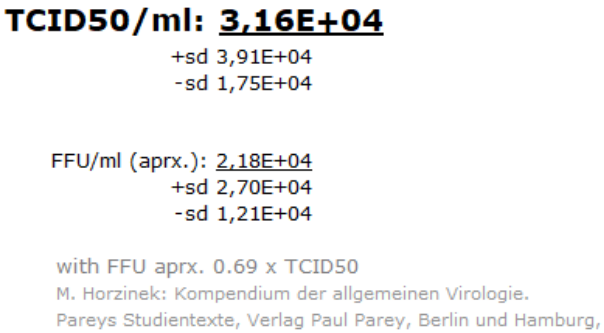

Figure 4.5.2: Values from $TCID_{50}$ calculator for Batch 1, post scoring based on no. of wells showing presence or absence of CPE

Batch 2:

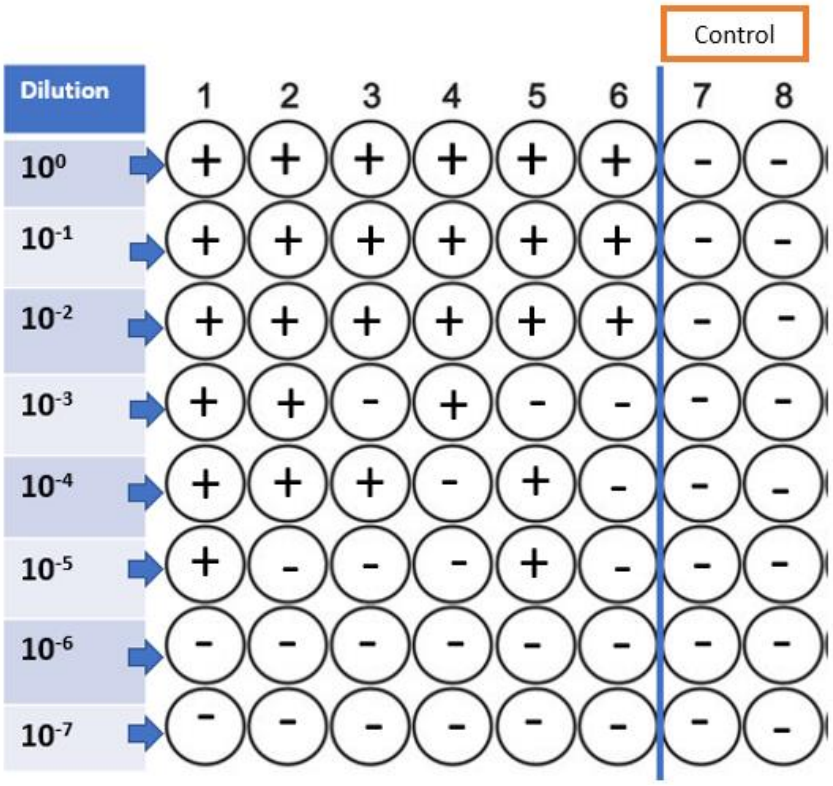

Figure 4.5.3: Figure indicating the layout overview for 2nd batch of viral titration, with cell scoring performed on day 14 post infection. '+' indicates approximately more than 50% of CPE associated cellular mortality. '-' indicates absence of CPE associated cell death.

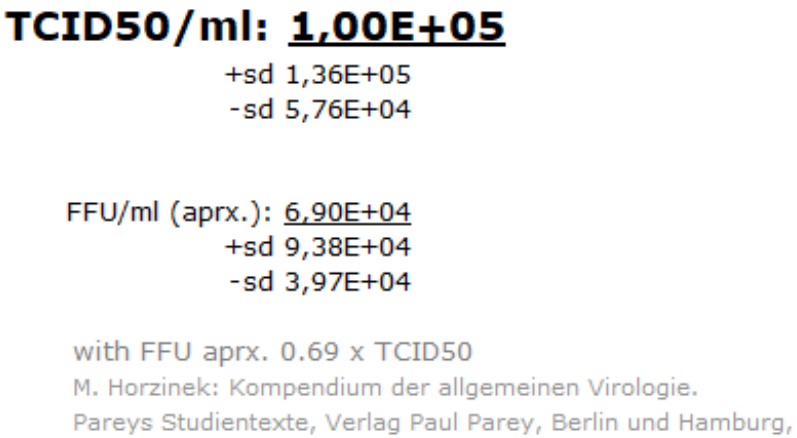

Figure 4.5.4: Values from $TCID_{50}$ calculator for Batch 2, post scoring based on no. of wells showing presence or absence of CPE.

Batch 3:

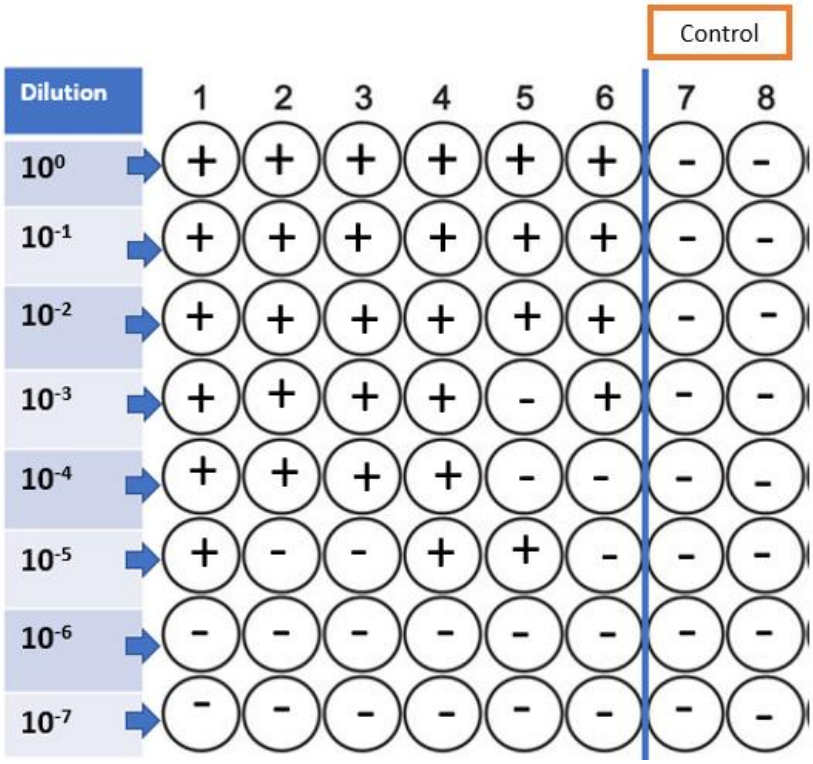

Figure 4.5.5: Figure indicating the layout overview for 3rd batch of viral titration, with cell scoring performed on day 14 post infection. '+' indicates approximately more than 50% of CPE associated cellular mortality. '-' indicates absence of CPE associated cell death.

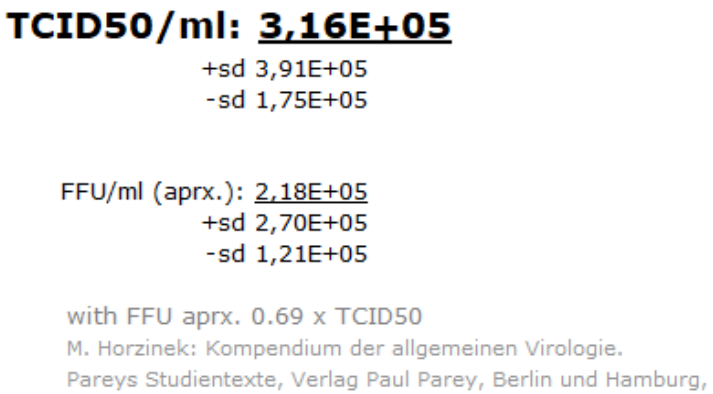

Figure 4.5.6: Values from $TCID_{50}$ calculator for Batch 3, post scoring based on no. of wells showing presence or absence of CPE

4.3.2 Calculations of FFU/ml and MOI

Post the virus titration, the goal is to calculate the viral titre. “A titre is defined as a given number of infectious viral units per unit volume”(Lei et al., 2020) .The calculations have been based on the principles by (Lei et al., 2020; Payne, 2017)

Using the TCID50 calculator we also get the value for FFU/ml which is approximately 0.69 * $TCID_{50}$/ml. Then we calculate FFU/ml in avg. for all the three batches.

That would be:

21800+ 69000 +218000 /3 = 102933.33333333.

Thus, the average value of FFU/ml is 102933.333 (post rounding off to three decimal units)

FFU/ml = 102933.333

This is the value of FFU per ml; in order to calculate the amount of FFU per well, we need value of FFU per 0.1 ml because we used 100 µl as the inoculum dose for ISAV inoculation/challenge for 10000 cells seeded per well in the 96 well plate (section **3.5.2**).

Therefore, 102933.333 * 0.1 = 10293.333. Thus,

FFU/well = 10293.333

MOI is equal to amount of amount of FFU/total no. of cells = 10293.333/10000 = 1.029. So,

MOI = 1.02

MOI = 1, which means approximately 1 virus particle infects 1 cell for our experimental setup.

So, in a culture with 10000 cells per well, 10000 viral particles are needed for the ISAV challenge which is approximately 100 microlitre for our virus sample. But however, 150 micro litre was used to ensure higher chances of infection of cell beyond the basal level. MOI of 1 is also consistent with other experimental works done on ISA virus (Svingerud et al., 2013, Schiøtz et al., 2009).

4.3.3 Virus challenge

An experiment of virus challenge was set up based on the result post virus titration and scoring as well as the analysis of knockout score post sample sequencing. The layout of the experiment has been explained in section **3.6**. The interpretation of result was based on the work by (B. Dannevig et al., 1995). The method of cell seeding and electroporation remined similar to section **3.3.4** and **3.5.2**. However, this time, based on the sequencing analysis, only the most effective guide in comparison was used for electroporation.

The set up involved three groups. First group was the infected knockout group which consisted of the SHK-1 cells with the specific gene knockout followed by virus inoculation. The control group consisted of healthy cells which were not challenged with the virus. The third group was the infected non-knockout group, which consisted of cells that did not have any gene editing in terms of gene knockout and were challenged with the ISAV inoculum.

Post infection, the cells were analysed for CPE on day 14. As we see in the images, all the wells showed presence of live cells, dead cells and cells with CPE except the control group which showed no CPE. Green circles have been used to indicate live healthy cells. Red circles have been used to indicate dead and or free-floating cells. White circles have been used to indicate the CPE as seen in SHK-1 cells post ISAV challenge, characterized by loss of adherence and increased cytoplasmic vacuolation in the cells (B. Dannevig et al., 1995).

However, depending on the treatment (i.e., Gene editing and virus inoculation) we aimed to study a pattern of variation within the degree of cellular mortality, CPE and density of live cells. Overall, the appearance of CPE seemed to be consistent with the time duration needed for development of prominent CPE by ISAV in SHK-1 cell lines (B. Dannevig et al., 1995; OIE, 2021). Overall, the results could not be considered conclusive enough and have been discussed in further detail in the section **5.2.3**.

gene *TMEM199*

The Infected knockout group showed lesser cellular mortality and CPE compared to the infected non-knockout group. The percentage of live cells in the Infected knockout group were however noticeably lesser compared to the control group. In comparison, the control group consisted of majority of live cells amongst the three groups, and lesser cellular mortality without any CPE, as expected. The infected non-knockout group showed presence of very few singular live cells and high degree of cellular mortality and virus induced CPE- characterized by cell death, loss of adherence and characteristic cytoplasmic vacuolation of the cells (B. Dannevig et al., 1995)

Figure 4.6.1. Image focusing on the live and dead cells observed in the Infected knockout group. **Figure 4.6.2**. Image focusing on the live and dead cells in control group. **Figure 4.6.3**. Image focusing on prominent CPE seen in non-knockout infected group

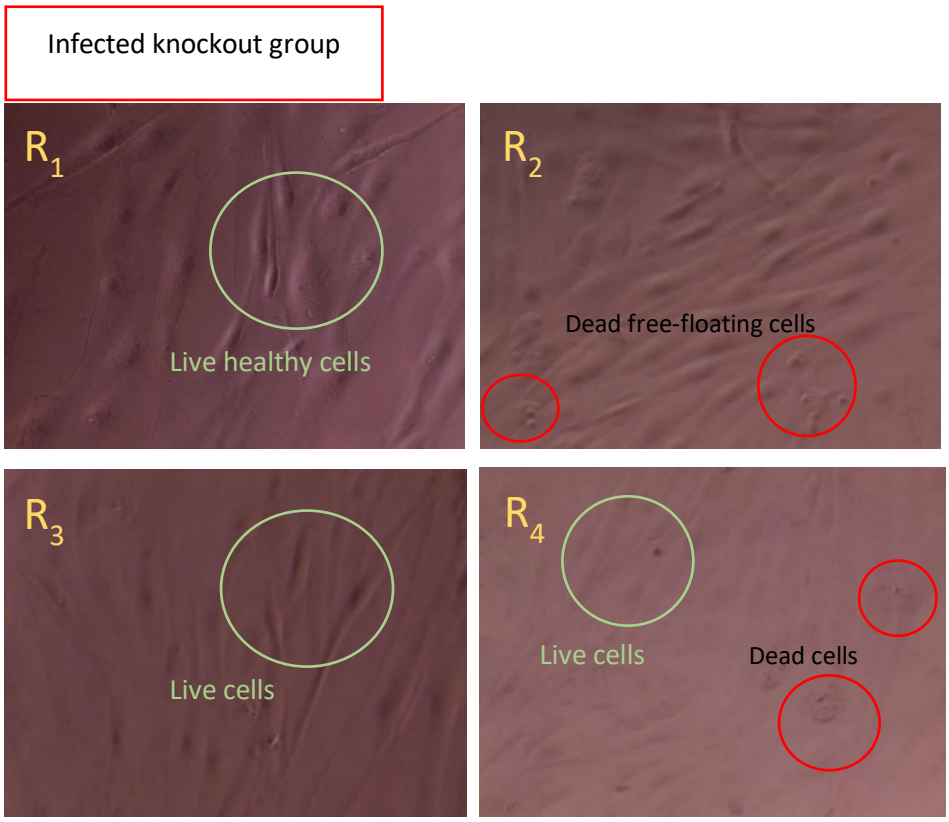

Figure 4.6.1

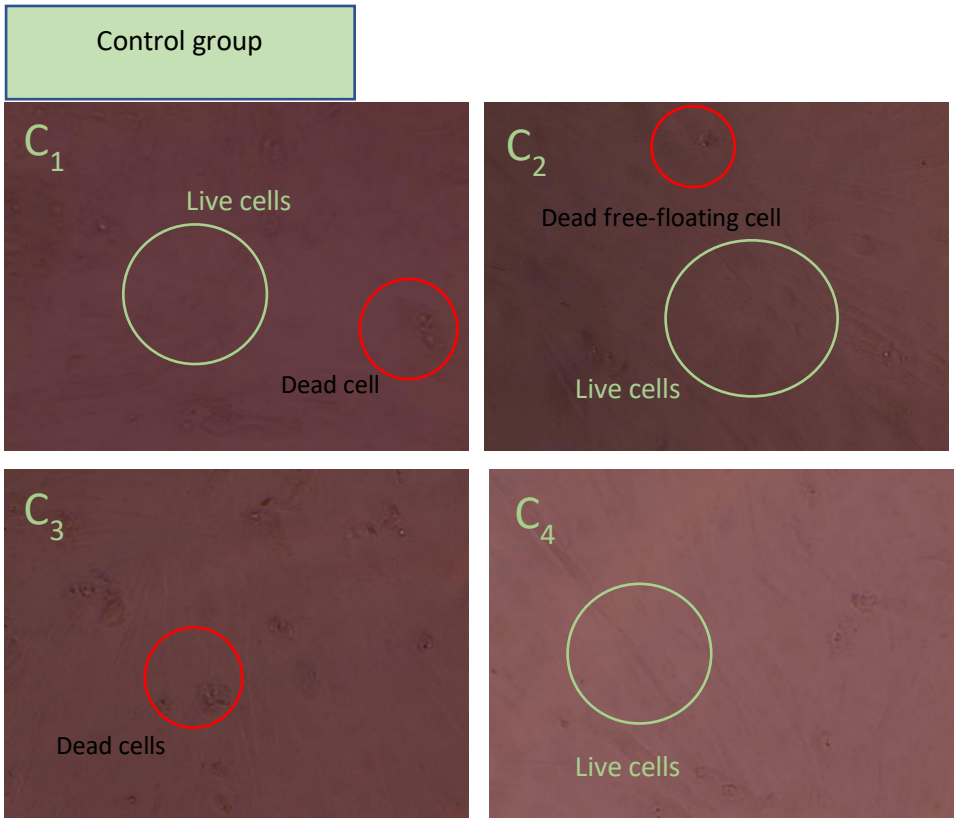

Figure 4.6.2

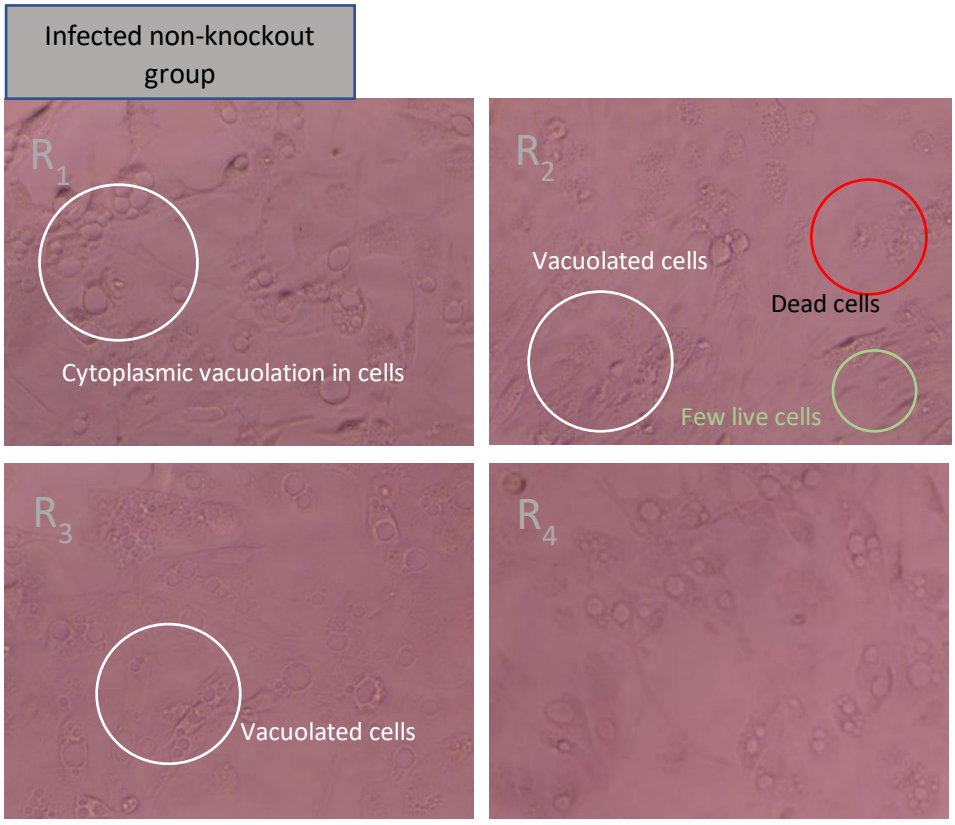

Figure 4.6.3

gene *WDR7*

The Infected knockout group for gene *WDR7* showed presence of high degree of cellular mortality and virus induced CPE, very similar to the infected non-knockout group. The control sample showed presence of a higher percentage of live cells compared to the other two groups along with few dead cells and no virus induced CPE, as we expected. However, replicate number 4 from Infected non-knockout group could not be analysed due to contamination in the well. The interpretation and detailed discussion of the result can be found in section **5.2.3**

Figure 4.7.1. Image focusing on the CPE in the Infected knockout group. **Figure 4.7.2**. Image focusing on the live and dead cells in control group **Figure 4.7.3**. Image focusing on prominent CPE seen in non-knockout infected group

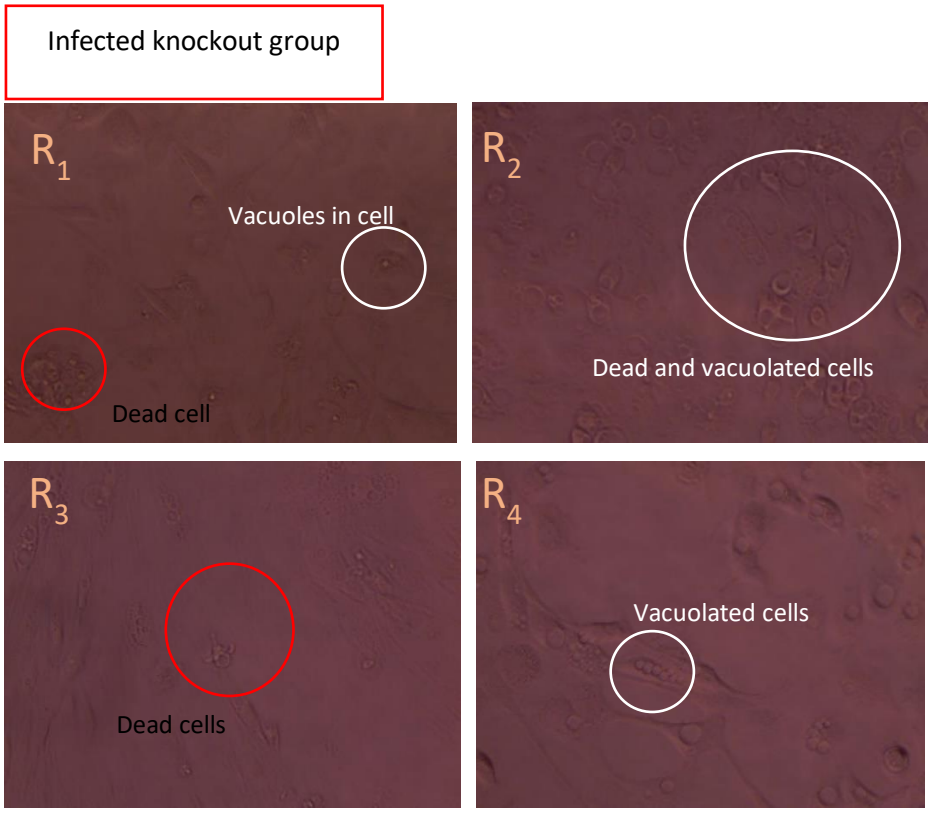

Figure 4.7.1

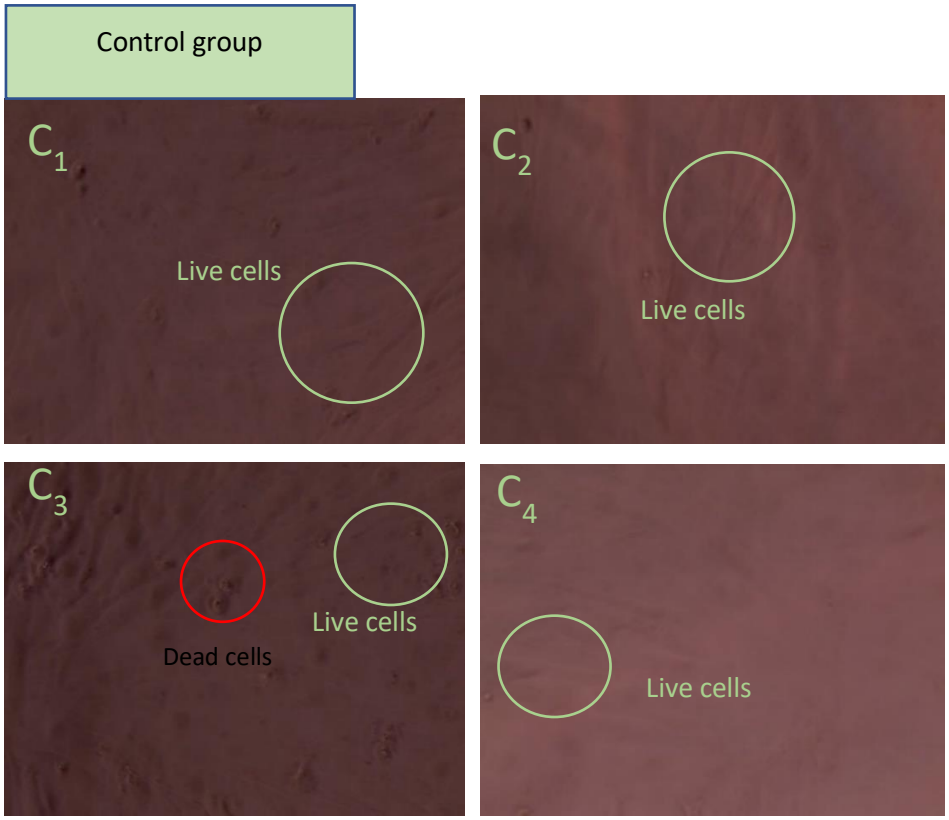

Figure 4.7.2

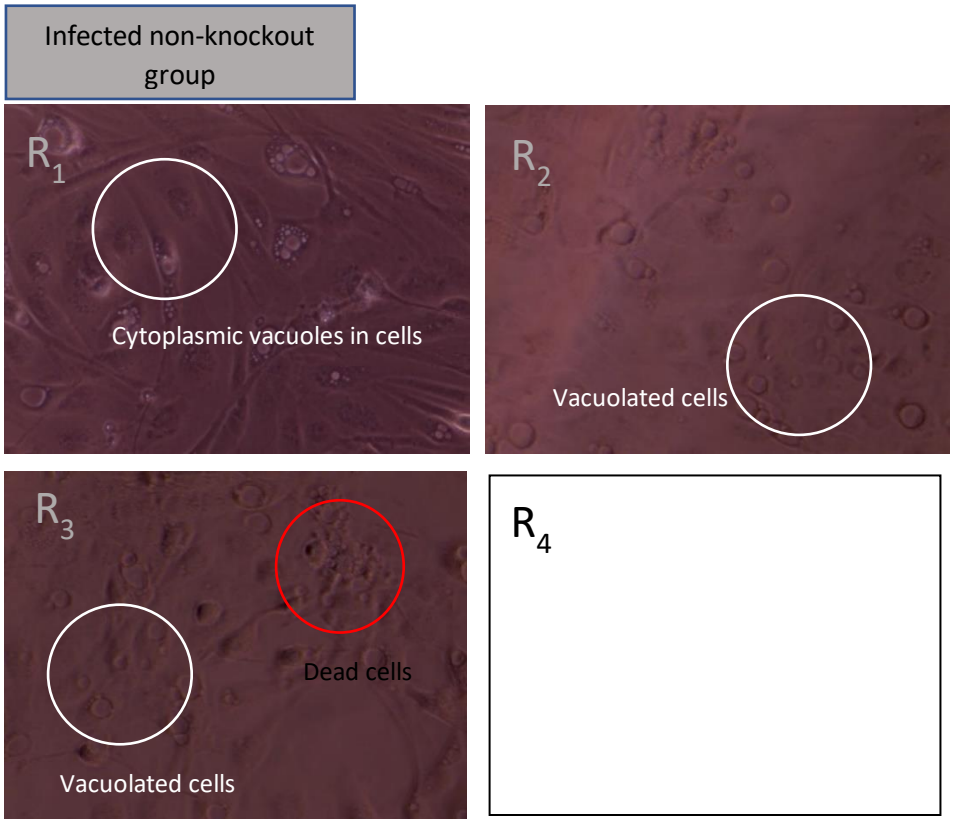

Figure 4.7.3

5 Discussion

5.1 Pre-Sequencing

5.1.1 Gene identification and guide RNA design.

Several factors like location, GC content, complementarity, number of mismatches and the efficiency percentage was considered while designing of the guide RNA. However, this experiment makes us realize the importance of placing special emphasis on gene duplications for a knock-out experiment. Designing of multiple potential guide RNAs would increase the probability of having an efficient guide RNA for gene knockout. A maximum of 2 guide RNAs were designed for the genes *CCDC115*, *WDR7* and *TMEM199* (**table 3.2**). The gene *CCDC115* did not show any duplications in its phylogenetic tree. Due to absence of duplications, emphasis was only placed on other parameters as discussed above. The gene *WDR7* and gene *TMEM199* showed one duplicate in its phylogenetic tree. Moving forward, the design of guide RNA in should be in such a way that it targets both the primary gene and its duplicate along with more careful and detailed analysis of the DNA sequences using alignment tools and protein characterizations (**7.3** Appendix - figures **7.3.1** and **7.3.2**). Gene duplications form an essential component of study especially in case of salmons, due to the WGD events.

5.1.2 Primer design, PCR and Agarose gel electrophoresis considerations

Primer design

Primer design was performed using the 'Primer Wizard' tool of the software Benchling as discussed before. The Benchling software was relatively user friendly and had a good interface. In case of the gene *CCDC115*, it was difficult to design primer pairs separately for the guide RNAs of choice due to their proximity and hence it was decided to design a single primer pair, with a view to cover both the guide RNAs that were designed for this particular gene (table **3.2**). The efficiency of the designed primers can be tested using the agarose gel electrophoresis, as discussed in section **4.1.2**.

Polymerase chain reaction

PCR reaction constitutes an important step in amplification of DNA and ensuring effective primer design. Failure to visualize bands in gel electrophoresis may indicate an error in the PCR protocol, contamination, or error in sample preparation, it may also be caused due to an ineffective primer.

The positive control sample that was used in this experiment was a previously designed and tested primer in Sandvik group for the gene *SLC45A2* based on the work by Edvardsen et al., (2014). Initial PCR protocol was followed using the Thermo Scientific™ PCR Master Mix (2X) kit and temperature settings as specified in the user manual for the same kit. However, the results were variable at different times and hence we decided to try the Platinum II Hot-Start Green PCR Master Mix kit (Thermo Scientific™). The use of this PCR master mix, eliminated the addition of dNTPs and Taq Polymerase enzyme, compared to the previous PCR kit protocol. In retrospective, failure of PCR in the previous PCR protocol could be attributed to one of the reagents used for sample preparation being ineffective. It is important to ensure optimum temperature settings for storage of reagents and also, while working in the laboratory. This step has helped us emphasize on maintaining ideal temperature conditions for sensitive reagents especially when working with multiple samples at a time and ensuring that the reagents are effective and stored well. PCR kits which require minimum number of steps or lesser reagents may be preferred over others depending on the nature of experiments, as a matter of preference.

5.2 Post sequencing

5.2.1 Sequencing analysis

Based on sequencing analysis, we saw very varied results for our samples. In case of knockout for gene *WDR7*, the knockout score was very less (6%). For the gene *CCDC115*, the quality score of samples were below the threshold limit and hence could not be analysed. However, we achieved a very high knockout score (98%) for the gene *TMEM199*. This translates to high efficiency of transfection of the cells and extremely efficient guide RNA; however, we need to perform more sequencing analysis in order to establish this gRNA as an

effective guide for knockout of the gene *TMEM199* for all future experiments. Moving forward, in case of gene *WDR7* we must design a gRNA taking into consideration the duplicate gene as well. The gene *CCDC115* does not have a duplicate gene and we must first reanalyse the sample for gRNA efficiency and then determine if it warrants re-designing of gRNA based on knockout score. It is also worth emphasizing on the importance of having sufficient number of replicate samples per gene and preparing samples with minimal error prior to sequencing. Another important aspect to consider is the cell culture passage number. In general, higher passage number could be associated with lower the transfection efficiency (de los Milagros Bassani Molinas et al., 2014). In our experiment, the cells were obtained from a cell culture passage number of 8. Further studies are needed to assess if passage number of cell culture has significant effect on transfection efficiency especially in the context of established cell lines like SHK-1 compared to the primary cell cultures.

5.2.2 Virus titration and scoring

$TCID_{50}$ assay (50% tissue culture infective dose) is a popular and commonly used technique for viral titre estimation. The median $TCID_{50}$ can be defined as the amount of dilution of the virus which is needed for infecting 50% of a given cell culture (Lei et al., 2020).

For our experiment, prior to the main experimental ISAV titration, two separate titrations were performed to assess if any difference exists between a fresh batch of viral inoculum for challenge and using a frozen viral inoculum. No considerable difference was found between the two batches and therefore it was decided to go ahead with the frozen vials of virus harvested from the same batch, for every virus challenge, assuming that it will ensure uniformity in terms of virus concentration in the inoculum. Another challenge that we faced was progressive evaporative loss of cell culture media in several of the well plates during incubation, a solution to which was to place the 96 well plates in airtight zip-lock plastic cover prior to being placed in the incubator.

The primary principle of $TCID_{50}$ lies in serial dilution of virus followed by determination of 50% end point dilution by observation of CPE under the microscope. Based on this, we realize that this method is prone to subjective errors and biases associated with misidentification of CPE between the wells of same or different dilutions. If performed error free, this method can be a good approximation for virus titre but not a definitive one. In our

case, statistically, based on the values of standard deviation (figure **4.5.2**, figure **4.5.4** and figure **4.5.6**), we see that the values in sample set are dispersed or spread out, thus indicting a lower reliability. A work by Pourianfar et al., (2012), attempts to eliminate the need for CPE observation by using a colorimetric method, thus reducing the subjective error. On titration of Enterovirus 71 (EV71), using MTS or MTT reagent for staining, with a modified method of virus dilution based on colorimetric approach, there was a reduction in time needed for the assay and it also improved the accuracy, reproducibility and subjectivity of results compared to the conventional $TCID_{50}$ approach ($p<0.01$) (Pourianfar et al., 2012).

According to Cresta D, Smith A. M. et al., (2021), the commonly used methods for the estimation of $TCID_{50}$ based on the outcome of the assay produce approximations that are biased; they introduce a measurement unit called Specific Infection (SIN) which is corresponding to the number of infections that the virus sample will cause and can be directly used to achieve the desired MOI and its calculation from end point assay does not need any changes in the experimental protocol and is done via a web-application called midSIN. The analysis of respiratory syncytial virus and influenza virus samples using midSIN showed that SIN/ml corresponded to the number of infections that will be caused by a sample, per ml, with their estimates showing more accuracy than Reed-Muench and Spearman-Kärber approximations (Cresta D, Smith A. M. et al., 2021), the latter of which is used in our experiment.

Some of the other limitations that we faced involve the time and effort associated with maintenance of cell lines and risk of contaminations, along with difficulty in interpretation of CPE etc., as also mentioned by Rolland et al., (2005).

5.2.3 Virus challenge study

Post quantitation of viral titre, the next part of the experiment was virus challenge study, which involved infecting/challenging of the experimental groups (infected knockout group and the non-knockout infected group) SHK-1 cells with quantified virus titre of ISAV inoculum. Overall, the result from the experiment provides a preliminary framework that helps us identify a pattern which should be analysed further for confirmation.

Gene *WDR7*

Based on the figures **4.7.1, 4.7.2 and 4.7.3,** we see that the *WDR7* knockout group with ISAV challenge showed high degree of CPE and cell mortality, similar to the infected non-knockout group. In a situation, where gene *WDR7* plays an essential role in ISAV pathogenesis without any another gene having a compensatory function and a knockout experiment with minimal error, we should be seeing higher number of live cells compared to the non-knockout infected group. However, in our case, the high amount of CPE and cell death may be attributed to an ineffective gRNA design and/or transfection, presence of a functional duplicate gene, genetic compensation etc. Control group, as expected, did not show any CPE due to absence of challenge with virus, but however, did show presence of dead free-floating cells. The images of control group also need to be focused better under the microscope.

Gene *TMEM199*

Based on the figures **4.6.1, 4.6.2 and 4.6.3,** we see that, interestingly, for the gene *TMEM199*, the infected knockout group has higher amount of visibly healthy cells compared to the infected non-knockout group. The infected non-knockout group showed characteristic CPE and high cellular mortality. The control group, did not show any CPE, as expected. It is important to note that, the infected knockout group also showed presence of CPE and dead cells (the microscopic field showing healthy cells has been focused in figure **4.6.1**), though not as distinct as the infected non-knockout group, this may be due to absence of gene knockout in the cells showing CPE. Our result points towards a certain pattern, for the infected knockout group for the gene *TMEM199*. The gene *TMEM199* is a necessary component for endosomal acidification in cells (Miles et al., 2017) and in case of ISAV, the viral and host cellular membrane fusion occurs in endosomal acidic environment (Eliassen et al., 2000), based on this information, we can postulate that knockout of the gene *TMEM199* might have led to a disruption of the endosomal pH gradient just enough for the cells to survive but prevented the viral membrane fusion, thus inhibiting infection, characterized by the presence of higher number of live cells in the infected knockout group.

Prior to undertaking a virus challenge experiment, it is important to study the duplicate genes and their possible functions in detail. The difficulty associated with this, lies in the fact that limited information is available about these duplicate genes. Another consideration would be to have an efficient CRISPR/Cas9 setup for gene editing. In case of transfection techniques, like electroporation, that we used in this particular experiment, it is important to consider the

effect of passage number of cell culture amongst other parameters. Moreover, a better understanding of the role of these genes could be achieved by using imaging techniques to visualize the stages of cellular pathogenesis and also quantification of the cell viability. In an experiment led by Bækkevold et al., (2009), to study cell viability assay of SHK-1 cells for studying cell death responses during ISAV infection, Cell Titer Blue assay - a fluorometric method, was used. Another interesting method to consider could be fluorescently labelling the virus. In a study led by Eliassen et al., (2000), fluorescently labelled viral particles were observed under confocal microscope, in order to investigate the initial steps involved with the interaction between ISAV and SHK-1 cells. Taking all these factors into consideration, a more efficient experiment can be set up in the future based on the framework and results achieved by this experiment.

5.2.4 Conclusion

This experiment was an attempt to investigate if at least one of the genes – *WDR7*, *CCDC115* and *TMEM199* played an essential role in development of ISAV infection in SHK-1 cell lines. These genes have not been studied before specifically in the context of ISAV infection in SHK-1 cells and hence, this thesis work involved optimization of many protocols and had challenges like availability of limited information and lack of sufficient previous research work to build upon. Based on our experimental work, the guide RNA that we designed for the gene *TMEM199*, enabled us to achieve a very high knockout score of 98%. Secondly, we were able to perform ISAV quantitation and thus determine the virus titre, which was then used in the virus challenge experiment; in order to better understand if the genes played an essential role in ISAV infection. The CRISPR/Cas9 based knockout followed by the virus challenge experiment for the gene *TMEM199* points towards a pattern which is also theoretically consistent with the infection mechanism of ISAV and hence warrants the consideration of *TMEM199* as a candidate gene for further analysis. In the future, consideration of the of the factors like - duplicate genes, genetic compensation, CRISPR/Cas9 delivery methods and better quantitation and imaging techniques for virus study, as discussed in the previous sections, will help us to develop a confirmatory analysis and thus establish the role of the concerned genes in ISAV infection conclusively. Even though this experiment did not conclusively establish the role of *TMEM199* in ISAV infection, it provided preliminary results which points towards the possibility of gene *TMEM199* playing an essential role in development of ISAV infection. Along with the consideration of several factors as discussed before, the results obtained in this experiment lays a strong structural framework that can be used to develop upon more in an effective manner for future experiments.

6 References

Aamelfot, M., Dale, O. B., & Falk, K. (2014). Infectious salmon anaemia – pathogenesis and tropism. *Journal of Fish Diseases*, *37*(4), 291–307. https://doi.org/10.1111/jfd.12225

Aamelfot, M., Dale, O. B., Weli, S. C., Koppang, E. O., & Falk, K. (2012). Expression of the infectious salmon anemia virus receptor on atlantic salmon endothelial cells correlates with the cell tropism of the virus. *Journal of Virology*, *86*(19), 10571–10578. https://doi.org/10.1128/JVI.00047-12

Asmamaw, M., & Zawdie, B. (2021). Mechanism and Applications of CRISPR/Cas-9-Mediated Genome Editing. *Biologics : Targets & Therapy*, *15*, 353–361. https://doi.org/10.2147/BTT.S326422

Bækkevold, E. S., Poulsen, L. C., Mjaaland, S., & Gjøen, T. (2009). Analysis of host- and strain-dependent cell death responses during infectious salmon anemia virus infection in vitro. *Virology Journal*, *6*(1), 91. https://doi.org/10.1186/1743-422X-6-91

Boyd, C. E., McNevin, A. A., & Davis, R. P. (2022). The contribution of fisheries and aquaculture to the global protein supply. *Food Security*, *14*(3), 805–827. https://doi.org/10.1007/s12571-021-01246-9

Cárdenas, M., Michelson, S., Pérez, D. R., Montoya, M., Toledo, J., Vásquez-Martínez, Y., & Cortez-San Martin, M. (2022). Infectious Salmon Anemia Virus Infectivity Is Determined by Multiple Segments with an Important Contribution from Segment 5. *Viruses*, *14*(3), 631. https://doi.org/10.3390/v14030631

Carr, C. M., Chaudhry, C., & Kim, P. S. (1997). Influenza hemagglutinin is spring-loaded by a metastable native conformation. *Proceedings of the National Academy of Sciences*, *94*(26), 14306–14313. https://doi.org/10.1073/pnas.94.26.14306

Chandrasekaran, A. P., Song, M., Kim, K.-S., & Ramakrishna, S. (2018). Different Methods of Delivering CRISPR/Cas9 Into Cells. *Progress in Molecular Biology and Translational Science*, *159*, 157–176. https://doi.org/10.1016/bs.pmbts.2018.05.001

Christiansen, D. H., McBeath, A. J. A., Aamelfot, M., Matejusova, I., Fourrier, M., White, P., Petersen, P. E., & Falk, K. 2017. (n.d.). First field evidence of the evolution from a non-virulent HPR0 to a virulent HPR-deleted infectious salmon anaemia virus. *Journal of General Virology*, *98*(4), 595–606. https://doi.org/10.1099/jgv.0.000741

Collet, B., Collins, C., & Lester, K. (2018). Engineered cell lines for fish health research. *Developmental & Comparative Immunology*, *80*, 34–40. https://doi.org/10.1016/j.dci.2017.01.013

Cook, J. D., Sultana, A., & Lee, J. E. (2017). Structure of the infectious salmon anemia virus receptor complex illustrates a unique binding strategy for attachment. *Proceedings of the National Academy of Sciences of the United States of America*, *114*(14), E2929–E2936. https://doi.org/10.1073/pnas.1617993114

Dannevig, B., Falk, K., & Press, C. (1995). Propagation of infectious salmon anaemia (ISA) virus in cell culture. *Veterinary Research*, *26*(5–6), 438–442.

Dannevig, B. H., Mjaaland, S., & Rimstad, E. (2008). Infectious Salmon Anemia Virus. In B. W. J. Mahy & M. H. V. Van Regenmortel (Eds.), *Encyclopedia of Virology (Third Edition)* (pp. 89–95). Academic Press. https://doi.org/10.1016/B978-012374410-4.00773-1

de los Milagros Bassani Molinas, M., Beer, C., Hesse, F., Wirth, M., & Wagner, R. (2014). Optimizing the transient transfection process of HEK-293 suspension cells for protein production by nucleotide ratio monitoring. *Cytotechnology*, *66*(3), 493–514. https://doi.org/10.1007/s10616-013-9601-3

Ditlecadet, D., Gautreau, C., Boston, L., Liston, R., Johnsen, E., & Gagné, N. (2022). First report of successful isolation of a HPR0-like variant of the infectious salmon anaemia virus (ISAV) using cell culture. *Journal of Fish Diseases*, *45*(3), 479–483. https://doi.org/10.1111/jfd.13556

Dong, W., & Kantor, B. (2021). Lentiviral Vectors for Delivery of Gene-Editing Systems Based on CRISPR/Cas: Current State and Perspectives. *Viruses*, *13*(7), 1288. https://doi.org/10.3390/v13071288

Edvardsen, R. B., Leininger, S., Kleppe, L., Skaftnesmo, K. O., & Wargelius, A. (2014). Targeted Mutagenesis in Atlantic Salmon (Salmo salar L.) Using the CRISPR/Cas9 System Induces Complete Knockout Individuals in the F0 Generation. *PLOS ONE*, *9*(9), e108622. https://doi.org/10.1371/journal.pone.0108622

Eliassen, T. M., Frøystad, M. K., Dannevig, B. H., Jankowska, M., Brech, A., Falk, K., Romøren, K., & Gjøen, T. (2000). Initial events in infectious salmon anemia virus infection: Evidence for the requirement of a low-pH step. *Journal of Virology*, *74*(1), 218–227. https://doi.org/10.1128/jvi.74.1.218-227.2000

Fitch, W. M. (1970). Distinguishing homologous from analogous proteins. *Systematic Zoology*, *19*(2), 99–113.

Fourrier, M., Lester, K., Thoen, E., Mikalsen, A., Evensen, Ø., Falk, K., Collet, B., & McBeath, A. (2014). Deletions in the highly polymorphic region (HPR) of infectious salmon anaemia virus HPR0 haemagglutinin-esterase enhance viral fusion and influence the interaction with the fusion protein. *The Journal of General Virology*, *95*(Pt 5), 1015–1024. https://doi.org/10.1099/vir.0.061648-0

Garneau, J. E., Dupuis, M.-È., Villion, M., Romero, D. A., Barrangou, R., Boyaval, P., Fremaux, C., Horvath, P., Magadán, A. H., & Moineau, S. (2010). The CRISPR/Cas

bacterial immune system cleaves bacteriophage and plasmid DNA. *Nature*, *468*(7320), 67–71. https://doi.org/10.1038/nature09523

Gervais, O., Barria, A., Papadopoulou, A., Gratacap, R. L., Hillestad, B., Tinch, A. E., Martin, S. A. M., Robledo, D., & Houston, R. D. (2021). Exploring genetic resistance to infectious salmon anaemia virus in Atlantic salmon by genome-wide association and RNA sequencing. *BMC Genomics*, *22*, 345. https://doi.org/10.1186/s12864-021-07671-6

Grant, R., & Smail, D. A. (n.d.). *Comparative isolation of infectious salmon anaemia virus (ISAV) from Scotland on TO, SHK-1 and CHSE-214 cells.* 6.

Gratacap, R. L., Jin, Y. H., Mantsopoulou, M., & Houston, R. D. (2020). *Efficient genome editing in multiple salmonid cell lines using ribonucleoprotein complexes* [Preprint]. Genetics. https://doi.org/10.1101/2020.04.03.022038

Gratacap, R. L., Regan, T., Dehler, C. E., Martin, S. A. M., Boudinot, P., Collet, B., & Houston, R. D. (2020). Efficient CRISPR/Cas9 genome editing in a salmonid fish cell line using a lentivirus delivery system. *BMC Biotechnology*, *20*(1), 35. https://doi.org/10.1186/s12896-020-00626-x

Håstein, T., Hellstrøm, A., Jonsson, G., Olesen, N. J., & Pärnänen, E. R.-. (2001). Surveillance of Fish Diseases in the Nordic Countries. *Acta Veterinaria Scandinavica*, *42*(1), S43. https://doi.org/10.1186/1751-0147-42-S1-S43

Håstein, T., Hill, B. J., & Winton, J. R. (1999). Successful aquatic animal disease emergency programmes. *Revue Scientifique et Technique (International Office of Epizootics)*, *18*(1), 214–227. https://doi.org/10.20506/rst.18.1.1161

Hellebø, A., Vilas, U., Falk, K., & Vlasak, R. (2004). Infectious salmon anemia virus specifically binds to and hydrolyzes 4-O-acetylated sialic acids. *Journal of Virology*, *78*(6), 3055–3062. https://doi.org/10.1128/jvi.78.6.3055-3062.2004

Hierholzer, J. C., & Killington, R. A. (1996). Virus isolation and quantitation. *Virology Methods Manual*, 25–46. https://doi.org/10.1016/B978-012465330-6/50003-8

Jaillon, O., Aury, J.-M., Brunet, F., Petit, J.-L., Stange-Thomann, N., Mauceli, E., Bouneau, L., Fischer, C., Ozouf-Costaz, C., Bernot, A., Nicaud, S., Jaffe, D., Fisher, S., Lutfalla, G., Dossat, C., Segurens, B., Dasilva, C., Salanoubat, M., Levy, M., … Roest Crollius, H. (2004). Genome duplication in the teleost fish Tetraodon nigroviridis reveals the early vertebrate proto-karyotype. *Nature*, *431*(7011), 946–957. https://doi.org/10.1038/nature03025

Jansen, M. D., Moldal, T., Dverdal, M., & Brun, E. (n.d.). *The surveillance programme for infectious salmon anaemia virus HPR0 (ISAV HPR0) in Norway 202*. 9.

Jinek, M., Chylinski, K., Fonfara, I., Hauer, M., Doudna, J. A., & Charpentier, E. (2012). A Programmable Dual-RNA–Guided DNA Endonuclease in Adaptive Bacterial Immunity. *Science*, *337*(6096), 816–821. https://doi.org/10.1126/science.1225829

Jinek, M., Jiang, F., Taylor, D. W., Sternberg, S. H., Kaya, E., Ma, E., Anders, C., Hauer, M., Zhou, K., Lin, S., Kaplan, M., Iavarone, A. T., Charpentier, E., Nogales, E., & Doudna, J. A. (2014). Structures of Cas9 endonucleases reveal RNA-mediated conformational activation. *Science (New York, N.Y.)*, *343*(6176), 1247997. https://doi.org/10.1126/science.1247997

Kasahara, M., Naruse, K., Sasaki, S., Nakatani, Y., Qu, W., Ahsan, B., Yamada, T., Nagayasu, Y., Doi, K., Kasai, Y., Jindo, T., Kobayashi, D., Shimada, A., Toyoda, A., Kuroki, Y., Fujiyama, A., Sasaki, T., Shimizu, A., Asakawa, S., … Kohara, Y. (2007). The medaka draft genome and insights into vertebrate genome evolution. *Nature*, *447*(7145), 714–719. https://doi.org/10.1038/nature05846

Kibenge, F. S. B., Kibenge, M. J. T., Wang, Y., Qian, B., Hariharan, S., & McGeachy, S. (2007). Mapping of putative virulence motifs on infectious salmon anemia virus

surface glycoprotein genes. *The Journal of General Virology*, *88*(Pt 11), 3100–3111. https://doi.org/10.1099/vir.0.83097-0

King, A. M. Q., Adams, M. J., Carstens, E. B., & Lefkowitz, E. J. (Eds.). (2012). Family—Orthomyxoviridae. In *Virus Taxonomy* (pp. 749–761). Elsevier. https://doi.org/10.1016/B978-0-12-384684-6.00061-6

Kjærner-Semb, E., Edvardsen, R. B., Ayllon, F., Vogelsang, P., Furmanek, T., Rubin, C. J., Veselov, A. E., Nilsen, T. O., McCormick, S. D., Primmer, C. R., & Wargelius, A. (2021). Comparison of anadromous and landlocked Atlantic salmon genomes reveals signatures of parallel and relaxed selection across the Northern Hemisphere. *Evolutionary Applications*, *14*(2), 446–461. https://doi.org/10.1111/eva.13129

Koonin, E. V. (2005). Orthologs, paralogs, and evolutionary genomics. *Annual Review of Genetics*, *39*, 309–338. https://doi.org/10.1146/annurev.genet.39.073003.114725

Kulshreshtha, V., Kibenge, M., Salonius, K., Simard, N., Riveroll, A., & Kibenge, F. (2010). Identification of the 3’ and 5’ terminal sequences of the 8 rna genome segments of european and north american genotypes of infectious salmon anemia virus (an orthomyxovirus) and evidence for quasispecies based on the non-coding sequences of transcripts. *Virology Journal*, *7*, 338. https://doi.org/10.1186/1743-422X-7-338

Lei, C., Yang, J., Hu, J., & Sun, X. (2020). On the Calculation of TCID50 for Quantitation of Virus Infectivity. *Virologica Sinica*, *36*(1), 141–144. https://doi.org/10.1007/s12250-020-00230-5

Li, B., Clohisey, S. M., Chia, B. S., Wang, B., Cui, A., Eisenhaure, T., Schweitzer, L. D., Hoover, P., Parkinson, N. J., Nachshon, A., Smith, N., Regan, T., Farr, D., Gutmann, M. U., Bukhari, S. I., Law, A., Sangesland, M., Gat-Viks, I., Digard, P., … Hacohen, N. (2020). Genome-wide CRISPR screen identifies host dependency factors for

influenza A virus infection. *Nature Communications*, *11*(1), 164. https://doi.org/10.1038/s41467-019-13965-x

Lien, S., Koop, B. F., Sandve, S. R., Miller, J. R., Kent, M. P., Nome, T., Hvidsten, T. R., Leong, J. S., Minkley, D. R., Zimin, A., Grammes, F., Grove, H., Gjuvsland, A., Walenz, B., Hermansen, R. A., von Schalburg, K., Rondeau, E. B., Di Genova, A., Samy, J. K. A., … Davidson, W. S. (2016). The Atlantic salmon genome provides insights into rediploidization. *Nature*, *533*(7602), 200–205. https://doi.org/10.1038/nature17164

MacLeod, M. J., Hasan, M. R., Robb, D. H. F., & Mamun-Ur-Rashid, M. (2020). Quantifying greenhouse gas emissions from global aquaculture. *Scientific Reports*, *10*(1), 11679. https://doi.org/10.1038/s41598-020-68231-8

Matrosovich, M., Herrler, G., & Klenk, H. D. (2013). Sialic Acid Receptors of Viruses. *SialoGlyco Chemistry and Biology II*, *367*, 1–28. https://doi.org/10.1007/128_2013_466

Miles, A. L., Burr, S. P., Grice, G. L., & Nathan, J. A. (2017). The vacuolar-ATPase complex and assembly factors, TMEM199 and CCDC115, control HIF1α prolyl hydroxylation by regulating cellular iron levels. *ELife*, *6*, e22693. https://doi.org/10.7554/eLife.22693

Moriyama, Y., & Koshiba-Takeuchi, K. (2018). Significance of whole-genome duplications on the emergence of evolutionary novelties. *Briefings in Functional Genomics*, *17*(5), 329–338. https://doi.org/10.1093/bfgp/ely007

Müller, A., Markussen, T., Drabløs, F., Gjøen, T., Jørgensen, T. Ø., Solem, S. T., & Mjaaland, S. (2010). Structural and functional analysis of the hemagglutinin-esterase of infectious salmon anaemia virus. *Virus Research*, *151*(2), 131–141. https://doi.org/10.1016/j.virusres.2010.03.020

Near, T. J., Eytan, R. I., Dornburg, A., Kuhn, K. L., Moore, J. A., Davis, M. P., Wainwright, P. C., Friedman, M., & Smith, W. L. (2012). Resolution of ray-finned fish phylogeny and timing of diversification. *Proceedings of the National Academy of Sciences of the United States of America*, *109*(34), 13698–13703. https://doi.org/10.1073/pnas.1206625109

Nylund, A., Plarre, H., Karlsen, M., Fridell, F., Ottem, K. F., Bratland, A., & Sæther, P. A. (2007a). Transmission of infectious salmon anaemia virus (ISAV) in farmed populations of Atlantic salmon (Salmo salar). *Archives of Virology*, *152*(1), 151–179. https://doi.org/10.1007/s00705-006-0825-9

Nylund, A., Plarre, H., Karlsen, M., Fridell, F., Ottem, K. F., Bratland, A., & Sæther, P. A. (2007b). Transmission of infectious salmon anaemia virus (ISAV) in farmed populations of Atlantic salmon (Salmo salar). *Archives of Virology*, *152*(1), 151–179. https://doi.org/10.1007/s00705-006-0825-9

Payne, S. (2017). Chapter 4—Methods to Study Viruses. In S. Payne (Ed.), *Viruses* (pp. 37–52). Academic Press. https://doi.org/10.1016/B978-0-12-803109-4.00004-0

Pérez, L., & Carrasco, L. (1993). Entry of poliovirus into cells does not require a low-pH step. *Journal of Virology*, *67*(8), 4543–4548. https://doi.org/10.1128/JVI.67.8.4543-4548.1993

Pourianfar, H. R., Javadi, A., & Grollo, L. (2012). A Colorimetric-Based Accurate Method for the Determination of Enterovirus 71 Titer. *Indian Journal of Virology : An Official Organ of Indian Virological Society*, *23*(3), 303–310. https://doi.org/10.1007/s13337-012-0105-0

Ramly, R. B., Olsen, C. M., Braaen, S., & Rimstad, E. (2013). Infectious salmon anaemia virus nuclear export protein is encoded by a spliced gene product of genomic segment 7. *Virus Research*, *177*(1), 1–10. https://doi.org/10.1016/j.virusres.2013.07.001

Redman, M., King, A., Watson, C., & King, D. (2016). What is CRISPR/Cas9? *Archives of Disease in Childhood. Education and Practice Edition*, *101*(4), 213–215. https://doi.org/10.1136/archdischild-2016-310459

Reinertsen, H., & Haaland, H. (1995). *Sustainable Fish Farming*. CRC Press.

Rimstad, E., & Markussen, T. (2020). Infectious salmon anaemia virus-molecular biology and pathogenesis of the infection. *Journal of Applied Microbiology*, *129*(1), 85–97. https://doi.org/10.1111/jam.14567

Rolland, J. B., Bouchard, D., Coll, J., & Winton, J. R. (2005). Combined use of the ASK and SHK-1 cell lines to enhance the detection of infectious salmon anemia virus. *Journal of Veterinary Diagnostic Investigation: Official Publication of the American Association of Veterinary Laboratory Diagnosticians, Inc*, *17*(2), 151–157. https://doi.org/10.1177/104063870501700209

Samy, J. K. A., Mulugeta, T. D., Nome, T., Sandve, S. R., Grammes, F., Kent, M. P., Lien, S., & Våge, D. I. (2017). SalmoBase: An integrated molecular data resource for Salmonid species. *BMC Genomics*, *18*(1), 482. https://doi.org/10.1186/s12864-017-3877-1

Sander, J. D., & Joung, J. K. (2014). CRISPR-Cas systems for editing, regulating and targeting genomes. *Nature Biotechnology*, *32*(4), 347–355. https://doi.org/10.1038/nbt.2842

Sandvik, T., Rimstad, E., & Mjaaland, S. (2000). The viral RNA 3'- and 5'-end structure and mRNA transcription of infectious salmon anaemia virus resemble those of influenza viruses. *Archives of Virology*, *145*(8), 1659–1669. https://doi.org/10.1007/s007050070082

Scott, C. J. W., Morris, P. C., & Austin, B. (2011). CELLULAR, MOLECULAR, GENOMICS, AND BIOMEDICAL APPROACHES | Molecular Fish Pathology. In

A. P. Farrell (Ed.), *Encyclopedia of Fish Physiology* (pp. 2032–2045). Academic Press. https://doi.org/10.1016/B978-0-12-374553-8.00037-X

Shao, M., Xu, T.-R., & Chen, C.-S. (2016). The big bang of genome editing technology: Development and application of the CRISPR/Cas9 system in disease animal models. *Dong Wu Xue Yan Jiu = Zoological Research*, *37*(4), 191–204. https://doi.org/10.13918/j.issn.2095-8137.2016.4.191

Smith, J. J., Kuraku, S., Holt, C., Sauka-Spengler, T., Jiang, N., Campbell, M. S., Yandell, M. D., Manousaki, T., Meyer, A., Bloom, O. E., Morgan, J. R., Buxbaum, J. D., Sachidanandam, R., Sims, C., Garruss, A. S., Cook, M., Krumlauf, R., Wiedemann, L. M., Sower, S. A., … Li, W. (2013). Sequencing of the sea lamprey (Petromyzon marinus) genome provides insights into vertebrate evolution. *Nature Genetics*, *45*(4), 415–421, 421e1-2. https://doi.org/10.1038/ng.2568

Svingerud, T., Holand, J. K., & Robertsen, B. (2013). Infectious salmon anemia virus (ISAV) replication is transiently inhibited by Atlantic salmon type I interferon in cell culture. *Virus Research*, *177*(2), 163–170. https://doi.org/10.1016/j.virusres.2013.08.004

Toennessen, R., Lauscher, A., & Rimstad, E. (2009a). Comparative aspects of infectious salmon anemia virus, an orthomyxovirus of fish, to influenza viruses. *Indian Journal of Microbiology*, *49*(4), 308–314. https://doi.org/10.1007/s12088-009-0055-4

Toennessen, R., Lauscher, A., & Rimstad, E. (2009b). Comparative aspects of infectious salmon anemia virus, an orthomyxovirus of fish, to influenza viruses. *Indian Journal of Microbiology*, *49*(4), 308–314. https://doi.org/10.1007/s12088-009-0055-4

Zhang, S., Shen, J., Li, D., & Cheng, Y. (2021). Strategies in the delivery of Cas9 ribonucleoprotein for CRISPR/Cas9 genome editing. *Theranostics*, *11*(2), 614–648. https://doi.org/10.7150/thno.47007

Reports and website reference list:

Abdullah Sami Madhun, Ørjan Karlsen, Rune Nilsen and Bjørn Olav Kvamme (IMR)(2021), Annual report on health monitoring of wild anadromous salmonids in Norway 2021. (2021). Retrieved 5 August 2022, from https://www.hi.no/hi/nettrapporter/rapport-fra-havforskningen-en-2022-6

FAO. 2022. The State of World Fisheries and Aquaculture 2022. Towards Blue Transformation. *Rome, FAO. https://doi.org/10.4060/cc0461en*

Jansen, Mona Dverdal, Silva de Oliveira, Victor Henrique. Surveillance for infectious salmon anaemia virus (ISAV HPRdel) in containment areas in Norway 2020. Report 54/2021. Veterinærinstituttet 2021.

OIE, World Organization for Animal Health (2021), Manual of diagnostic tests for Aquatic animals, chapter 2.3.4, p:282-293) url: https://www.woah.org/fileadmin/Home/fr/Health_standards/aahm/current/2.3.04_ISAV.pdf

Philippe Le Mercier, P. (2022). Isavirus ~ ViralZone. Retrieved 13 August 2022, from https://viralzone.expasy.org/95

Record high Norwegian seafood exports in 2021. (2022). Retrieved 13 August 2022, from https://en.seafood.no/news-and-media/news-archive/record-high-norwegian-seafood-exports-in-2021/

7 Appendices

7.1 Appendix: Abbreviations

Table 7.1: Commonly used abbreviations

2 ME	2 - Mercaptoethanol
bp	base pair
CCDC115	Coiled-coil containing domain 115
CPE	Cytopathogenic effect
DNA	Deoxyribonucleic acid
FAO	Food and Agriculture Organization
FBS	Fetal Bovine Serum
FFU	Focus forming units
gRNA	Guide RNA
ISAV	Infectious salmon anemia virus
Kb	kilobase
MOI	Multiplicity of infection
MTS	3-(4,5-dimethylthiazol-2-yl)-5-(3-carboxymethoxyphenyl)-2-(4-sulfophenyl)-2H-tetrazoli
MTT	3-(4, 5-dimethylthiazol-2-yl)-2, 5-diphenyltetrazolium bromide
OIE	World Organization for Animal Health
PBS	Phosphate buffered saline
PCR	Polymerase Chain Reaction
Pen. Strep	Penicillin-streptomycin
p.i.	Post infection (with ISAV inoculum) *
RNA	Ribonucleic acid
SHK-1	Salmon head kidney cell line-1
SNP	Single nucleotide polymorphism
tm199 / TMEM199	Transmembrane protein 199
$TCID_{50}$	50% Tissue culture infective dose
WDR7	WD repeat domain 7

WGD	Whole Genome Duplication
WHO	World Health Organization
WT	Wild Type

***Relevant to our experiment**

7.2 Appendix: Reagents, equipment, and software

Table 7.2.1: Reagents used

Sr. number	Product	Manufacturer	Catalogue number
1.	2-Mercaptoethano	Gibco	31350010
2.	50X TAE Electrophoresis buffer B	Thermo Fisher Scientific	B49
3.	Agarose	Sigma	A9539
4.	Cell Counting Kit, 30 dual chambered slides, 60 counts, with trypan blue	Bio Rad	1450003
5.	ECACC General Cell Collection: SHK-1	European Collection of Authenticated Cell Cultures (ECACC)	97111106
6.	ExoSAP-IT™ Express PCR Product Cleanup Reagent	Applied Biosystems™ ThermoFisher Scientific	75001.1.EA
7.	Fetal Bovine Serum	Gibco	26400044
8.	GeneRuler 1 kb DNA Ladder	Thermo Fisher Scientific	SM0312
9.	Leibovitz's L-15 media	Gibco	11415064
10.	NEON™ Transfection Kit	Invitrogen	MPK1096K
11.	Nucleic Acid Staining Solution	Nordic BioSite	250-67A532
12.	Opti-MEM™ Reduced Serum Medium	Gibco	31985047
13.	Penicillin-streptomycin	Gibco	15140122
14.	Phosphate buffered saline	Gibco	20012027
15.	Platinum™ II Hot-Start Green PCR Master Mix (2X)	Invitrogen ThermoFisher Scientific	14001013
16.	QuickExtract™ DNA Extraction Solution	Lucigen	QE09050
17.	Trypsin-EDTA solution	Gibco	25200056

Table 7.2.2: Equipment used

Sr. number	Product
1.	NanoDrop 8000 Spectrophotometer
2.	Neon Transfection System
3.	TC-20 Automated cell counter
4.	The ChemiDoc XRS+ Gel Imaging System
5.	EVOS ™ XL Core Imaging system – ThermoFisher Scientific

Table 7.2.2: Software used

Sr.no	Software
1.	AliView alignment viewer and editor
2.	Image lab 6.0

7.3 Appendix: Data

FASTA file data for the genes have been attached as a pdf file.

Table 7.3.1: Table values indicating DNA concentration of each sample measured using Nanodrop.

Gene name	Replicate number	DNA concentration (ng/µl)
WDR7	1	34.05
	2	22.23
	3	69.26
	4	106.5
CCDC115	1	165.4
	2	93.95
	3	118.5
	4	57.40
TMEM199	1	124.7
	2	69.36
	3	73.00
	4	39.72
Wild type	1	92.98
	2	133.4
	3	261.6
	4	119.6

Table 7.3.2: Table showing the sample layout for gene *TMEM199*

Serial number	Replicate number	Sample ID	Primer pair number
1	1	FTW922	1
2	2	FTW921	1
3	3	FTW920	1
4	4	FTW919	1
5	1	FTW918	2
6	2	FTW917	2
7	3	FTW916	2
8	4	FTW913	2
9	Wild type for primer 1	FTW914	1
10	Wild type for primer 2	FTW915	2

Table 7.3.3: Table showing the sample layout for gene *WDR7*.

Serial number	Replicate number	Sample ID	Primer pair number
1	1	FTW937	1
2	2	FTW936	1
3	3	FTW935	1
4	4	FTW934	1
5	1	FTW933	2
6	2	FTW932	2
7	3	FTW931	2
8	4	FTW930	2
9	Wild type for primer 1	FTW929	1
10	Wild type for primer 2	FTW928	2

Table 7.3.4: Table showing the sample layout for gene *CCDC115*

Serial number	Replicate number	Sample ID	Primer pair number
1	1	FTW927	1
2	2	FTW926	1
3	3	FTW925	1
4	4	FTW924	1
5	Wild type for primer 1	FTW923	1

Table 7.3.5: Table showing the sample knockout analysis for gene *TMEM199*

Sample ID	Primer pair number	Knockout score
FTW922	1	98
FTW921	1	96
FTW920	1	-
FTW919	1	-
FTW918	2	-
FTW917	2	-
FTW916	2	-
FTW913	2	-

'-' indicates a low-quality score for sample

Table 7.3.3: Table showing the sample knockout analysis for gene *WDR7*.

Sample ID	Primer pair number	Knockout score
FTW937	1	5
FTW936	1	6
FTW935	1	-
FTW934	1	-
FTW933	2	-
FTW932	2	-
FTW931	2	-
FTW930	2	-

'-' indicates a low-quality score for sample

Table 7.3.4: Table showing the sample knockout analysis for gene *CCDC115*

Sample ID	Primer pair number	Knockout score
FTW927	1	-
FTW926	1	-
FTW925	1	-
FTW924	1	-

'-' indicates a low-quality score for sample

Gene *TMEM199*

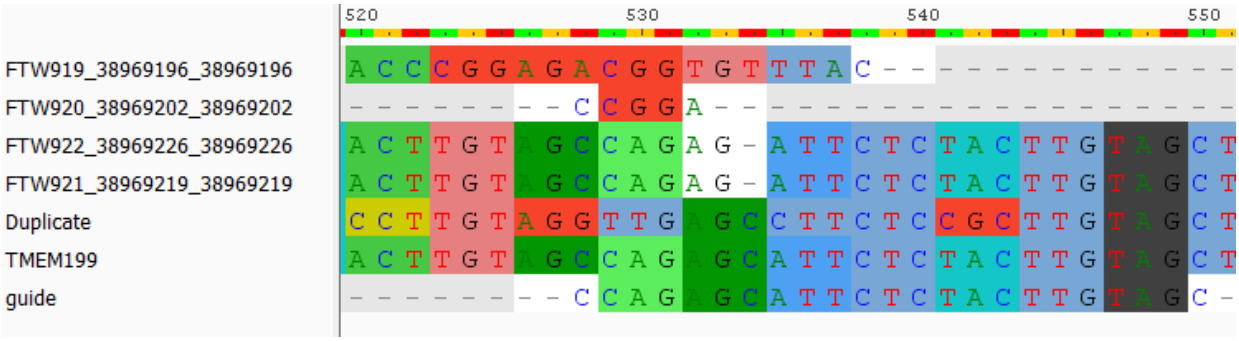

Figure 7.3.1: Image showing the translated nucleotides to amino acid sequences at the region of guide RNA, using AliView alignment viewer

Gene *WDR7*

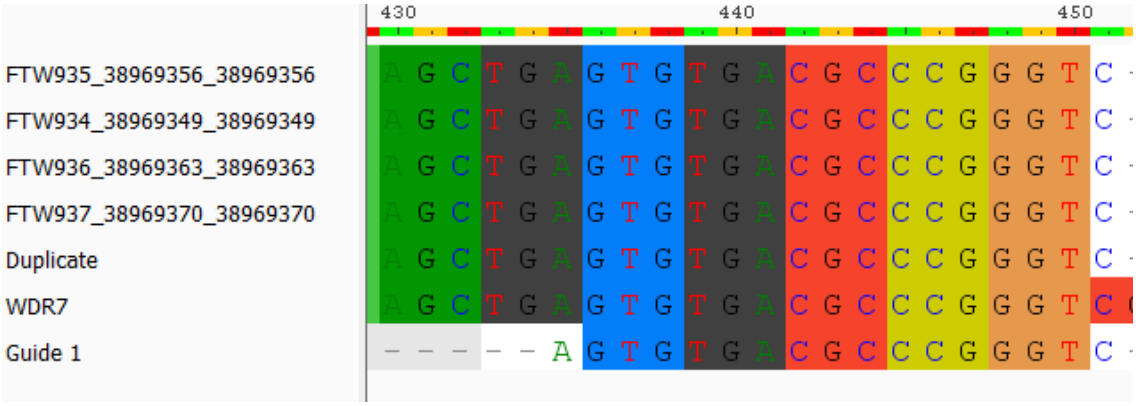

Figure 7.3.1: Image showing the translated nucleotides to amino acid sequences at the region of guide RNA, using AliView alignment viewer

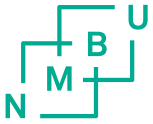

Norges miljø- og biovitenskapelige universitet
Noregs miljø- og biovitskapelege universitet
Norwegian University of Life Sciences

Postboks 5003
NO-1432 Ås
Norway